Inorganic Chemistry

pubs.acs.org/IC

Article

Mesoionic Carbenes in Low- to High-Valent Vanadium Chemistry

Florian R. Neururer, Shenyu Liu, Daniel Leitner, Marc Baltrun, Katherine R. Fisher, Holger Kopacka, Klaus Wurst, Lena J. Daumann, Dominik Munz,* and Stephan Hohloch*

Cite This: *Inorg. Chem.* 2021, 60, 15421−15434

Read Online

ACCESS | Metrics & More | Article Recommendations | Supporting Information

ABSTRACT: We report the synthesis of vanadium(V) oxo complex **1** with a pincer-type dianionic mesoionic carbene (MIC) ligand $\mathbf{L^1}$ and the general formula $[VOCl(L^1)]$. A comparison of the structural (SC-XRD), electronic (UV−vis), and electrochemical (cyclic voltammetry) properties of **1** with the benzimidazolinylidene congener **2** (general formula $[VOCl(L^2)]$) shows that the MIC is a stronger donor also for early transition metals with low d-electron population. Since electrochemical studies revealed both complexes to be reversibly reduced, the stronger donor character of MICs was not only demonstrated for the vanadium(V) but also for the vanadium(IV) oxidation state by isolating the reduced vanadium(IV) complexes $[\mathbf{Co(Cp^*)_2}][\mathbf{1}]$ and $[\mathbf{Co(Cp^*)_2}][\mathbf{2}]$ ($[Co(Cp^*)_2]$ = decamethylcobaltocenium). The electronic structures of the compounds were investigated by computational methods. Complex **1** was found to be a moderate precursor for salt metathesis reactions, showing selective reactivity toward phenolates or secondary amides, but not toward primary amides and phosphides, thiophenols, or aryls/alkyls donors. Deoxygenation with electron-rich phosphines failed to give the desired vanadium(III) complex. However, treatment of the deprotonated ligand precursor with vanadium(III) trichloride resulted in the clean formation of the corresponding MIC vanadium(III) complex **6**, which undergoes a clean two-electron oxidation with organic azides yielding the corresponding imido complexes. The reaction with TMS-N_3 did not afford a nitrido complex, but instead the imido complex **10**. This study reveals that, contrary to popular belief, MICs are capable of supporting early transition-metal complexes in a variety of oxidation states, thus making them promising candidates for the activation of small molecules and redox catalysis.

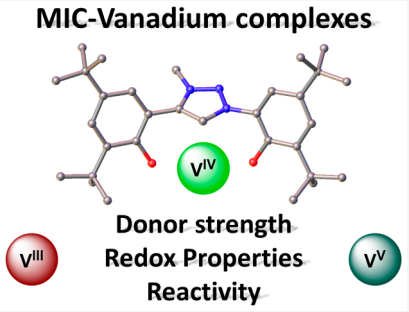

INTRODUCTION

Almost two decades after the first report of an abnormal 5-imidazolinylidene carbene complex,[1] mesoionic carbenes have been developed into a distinguished ligand class.[2,3] Among them, 1,2,3-triazole derived mesoionic carbenes, namely 1,2,3-triazolinylidenes,[4] stand out by their modular synthesis via the copper-catalyzed [3 + 2] cycloaddition between azides and alkynes.[5−7] After their initial reporting by Albrecht *et al.*,[8] they quickly became prominent synthetic targets for (electro-) catalysis,[9−23] supramolecular chemistry,[24−27] magnetism,[28] and photochemistry due to their versatile synthesis and comparatively straightforward handling.[29−36] Throughout these studies, a great effort has been made to decipher their electronic structure. Mesoionic carbenes are commonly believed to be strong σ-donor ligands paralleling heteroaryls; however, recent reports emphasize their π-accepting properties[37−39] as demonstrated by the isolation of a reduced triazolinylidene ligand.[40] Nevertheless, most studies targeted hitherto late transition metals or main group elements, while early transition-metal complexes with mesoionic carbenes have been rarely explored.[41−44] Arguably, this can be attributed to the relatively weak bond between *N*-heterocyclic carbenes and early transition metals.[45] However, this weak bond may be enhanced by harnessing anionic linkers. This strategy has allowed the isolation of a number of interesting metal complexes[46−49] of the early transition metals,[50−71] the lanthanides,[72−80] and the actinides.[81−86]

Among the early transition metals, vanadium chemistry has witnessed a remarkable activity over the past 50 years and has been applied in heterogeneous and homogeneous catalysis,[87] small molecule activation,[88−92] molecular magnetism,[93−96] and spin qubits.[97−100] Narrowing down the field to NHC vanadium complexes, since the first two reports of vanadium NHC complexes in 1994 by Roesky *et al.*[101] and 2003 by Abernethy *et al.*,[102] the utility of these complexes has mostly been explored in polymerization catalysis.[103−107] Beyond this, only a few other applications of vanadium-NHC complexes have been examined, including small molecule activation[108,109] and the neutralization of chemical warfare agents.[110] Still, most vanadium NHC complexes refer to diamagnetic vanadium(V) complexes, while low-valent vanadium complexes have been rarely investigated.[101,106,111−114]

Received: July 9, 2021
Published: September 30, 2021

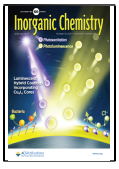

Inspired by Bellemin-Laponnaz's ligand design, employing two anionic redox-active phenolate linkers,[50−54,115−117] we have recently reported the first mesoionic carbene complexes of groups IV, V, and VI based on a 1,2,3-triazolinylidene scaffold.[44] Our initial report focused on niobium as a group V representative, and we thus expand this chemistry herein toward vanadium. We report the ligand's σ-donor strength by comparing the structural, spectroscopic, and electrochemical properties of the triazolinylidene complex **1** with its benzimidazolinylidene (benzNHC) congener **2**, proving the triazolinylidene ligand $\mathbf{L^1}$ as the stronger donor. Furthermore, the salt metathesis reactivity of the new triazolinylidene complex **1** is presented, revealing moderate scope. While phenols and secondary amides give good and clean conversion, all other nucleophiles investigated gave no tractable reaction products. We furthermore report on the isolation of various vanadium complexes in the oxidation states +IV and +III, where the latter are potent precursors to vanadium(V) imido complexes.

Scheme 1. Synthesis of the Vanadium(V) NHC Complexes Following Protonolysis between the Corresponding Azolium Salts and $VO(O^iPr)_3$

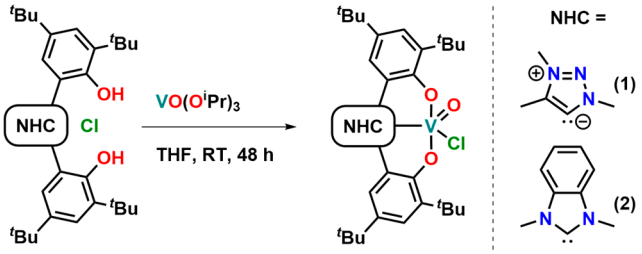

RESULTS AND DISCUSSION

Despite our previous finding that protonolysis between the triazolium salt $[\mathbf{H_3L^1}][\mathbf{Cl}]$ and $Ti(O^iPr)_3Cl$ did not lead to quantitative deprotonation of the triazolium salt,[44] we decided to adopt this strategy using $VO(O^iPr)_3$ as the vanadium source. To our delight, the reaction between the triazolium salt $[\mathbf{H_3L^1}][\mathbf{Cl}]$ and $VO(O^iPr)_3$, followed by the subsequent washing of the crude solids with hexane, afforded the MIC vanadium-oxo complex **1** as a dark green powder in yields of 85% (Scheme 1). The ^{1}H NMR spectrum of **1** in benzene confirmed the desired transformation due to the absence of the O*H* and triazolium-5*H* protons which revealed a C_1 symmetric species in solution. Unfortunately, due to the high quadrupolar moment of the ^{51}V nucleus, we were not able to observe the characteristic ^{13}C NMR resonance of the triazolinylidene carbon atom. Nevertheless, the absence of the triazolium-5*C* resonance at 131.9 ppm in the ^{13}C NMR of **1** confirms the formation of a triazolinylidene complex of high-valent vanadium(V). Furthermore, a shift of the ^{51}V resonance to −533 ppm (Figure S5) in the ^{51}V NMR indicates the presence of a strong donor ligand. To set this value into context, we also synthesized the benzimidazolinylidene complex **2**, recently reported by LeRoux et al.[118,119] The proton NMR of **2** shows a C_s symmetric species in solution where the absence of the O*H* and the benzimidazolium-2*H* protons indicates also the formation of an NHC complex of vanadium(V). Similar to **1**, we could not observe the carbene carbon resonance in the ^{13}C NMR spectrum of **2**. The ^{51}V NMR signal of **2** is (compared to complex **1**) strongly shifted to lower fields resonating at −503 ppm (Figure S10), indicating a lower donor strength of the benzimidazolinylidene compared to the triazolinylidene ligand.[120] Unambiguous proof for the formation of the NHC and MIC complexes was obtained by single-crystal X-ray diffraction (SC-XRD) analysis. X-ray quality crystals of **1** and **2** could be grown by slow diffusion of pentane into a concentrated solution of the corresponding complexes in toluene or benzene, respectively (Figure 2). Complex **1** crystallized in the monoclinic space group $P2_1/n$ as a toluene solvate, while complex **2** crystallized without additional solvent molecules in the asymmetric unit in the orthorhombic space group *Pbca*. The most striking difference in the molecular conformations of the complexes is that in the case of **2**, the benzannulated heterocycle is shifted out of plane compared to the C1−V1 bond axis by 16.7(1)°, while for the triazolinylidene complex **1**, this pitch angle along the C1−V1 bond axis was found to be only 0.7(1)°. These structural parameters are well reproduced by density functional theory (DFT) calculations (Table S1) and are also discernible in the coordination environment around the vanadium center. While **1** adopts an almost perfect square pyramidal coordination environment in the solid state (τ_5 = 0.05), complex **2** is distorted with τ_5 = 0.20. The C1−V1 distances in **1** and **2** are 2.055(3) Å and 2.131(3) Å, suggesting a stronger metal carbene interaction in **1** compared to **2**. This agrees with the pronounced high-field shift of the ^{51}V NMR resonances in **1** relative to **2**. The V1−O10 distances were determined to be 1.583(3) Å and 1.585(2) Å in **1** and **2**, showing only a minor influence of the NHC moiety toward the strength of the V═O bonds. However, the influence of the NHC unit on the V═O stretching frequencies in the IR is discernible with resonances at 986 cm^{-1} (calculated: 1026 cm^{-1}) and 1000 cm^{-1} (calculated: 1035 cm^{-1}) in **1** and **2**. These values are indicative for a weaker V═O multiple bond character in **1** in comparison to **2** due to arguably reduced π-donation from the terminal oxo ligand, and thus, corroborate stronger donor properties of the MIC ligand.

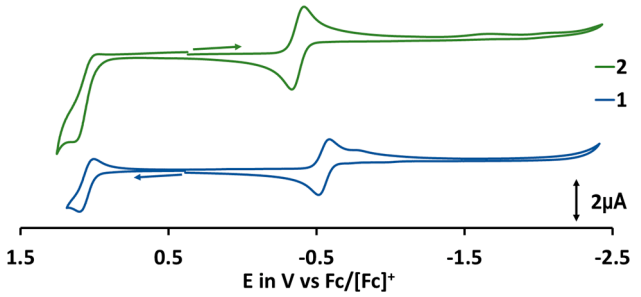

Figure 1. Cyclic voltammogram of **1** (blue) and **2** (green) in 0.1 M NBu_4PF_6 in CH_2Cl_2 at 298 K. Scan rate: 100 mV s^{-1}.

Table 1. Oxidation and Reduction Potentials of the Vanadium(V)-NHC Complexes 1 and 2 Referenced vs Fc/$[Fc]^+$ in 0.1 M NBu_4PF_6 Solutions in CH_2Cl_2 at 298 K

complex	$E^{1/2}$ ox. (V)	ΔE (mV)	$E^{1/2}$ red. (V)	ΔE (mV)
1	1.05	80	−0.56	70
2	n.a.	n.o.	−0.37	90

https://doi.org/10.1021/acs.inorgchem.1c02087
Inorg. Chem. 2021, 60, 15421−15434

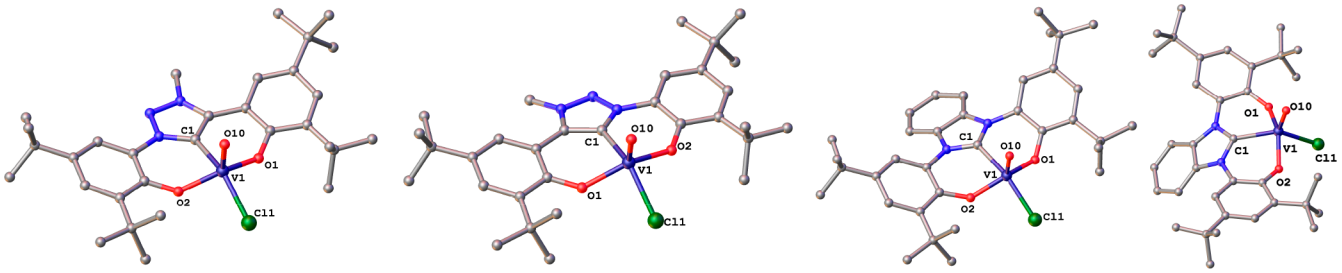

Figure 2. Molecular structures of **1**, [**Co(Cp*)$_2$**][**1**], **2**, and [**Co(Cp*)$_2$**][**2**] (from left to right). Hydrogen atoms, solvent molecules, and counterions have been omitted for clarity.

Scheme 2. Reduction of Complexes 1 and 2 by Decamethylcobaltocene

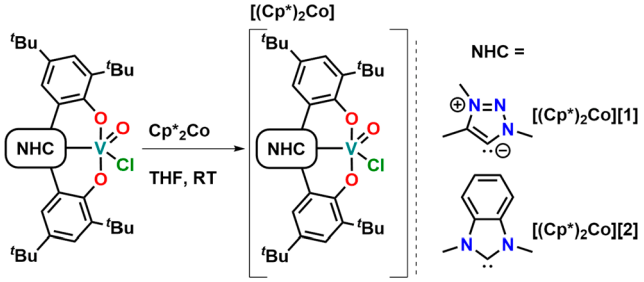

To further probe the donor properties of the triazolin- versus the benzimidazolinylidene donor, we investigated the complexes by electrochemical methods. Cyclic voltammetry measured in dichloromethane revealed a reversible reduction corresponding to the V(V/IV) redox couple for both complexes (Figure 1). In agreement with the results from ^{51}V NMR and IR spectroscopy, the reduction potential (the reductions are vanadium centered, *vide infra*) for **1** appears 0.19 V cathodically shifted compared to the reduction potential of **2** (Table 1). This suggests a higher electron density at the vanadium center in **1**, which is in line with the higher σ-donor character of MIC relative to benzNHC ligands. Additionally, complex **1** showed one reversible (ligand-centered) oxidation, whereas for **2** it is at the edge of the solvent window and thus could not be evaluated (Figures S69−S72).

To reveal the site of reduction for the two vanadium complexes, we reduced the complexes with decamethylcobaltocene (Scheme 2). While a THF solution turned greyish upon reduction of **1**, the desired product precipitated as a bright green powder for **2**. Evans method in CD_2Cl_2 revealed a magnetic moment of 1.74 and 1.67 μ_B for [**Co(Cp*)$_2$**][**1**] and [**Co(Cp*)$_2$**][**2**], which is in agreement with a vanadium(IV) redox state.[121] Accordingly, the V═O stretches shift from 986 to 932 cm^{-1} (calculated: 1026 to 1007 cm^{-1}) and from 1000 to 968 cm^{-1} (calculated: 1035 to 1007 cm^{-1}) in [**Co(Cp*)$_2$**][**1**] and [**Co(Cp*)$_2$**][**2**], respectively (see Figures S49−S52). X-ray quality crystals of both reduced complexes [**Co(Cp*)$_2$**][**1**] and [**Co(Cp*)$_2$**][**2**] could be grown by the slow evaporation of dichloromethane out of a hexane/dichloromethane mixture (Figure 2).

While the general structural factors (e.g., coordination environment) resemble the same trends as the parent vanadium(V) complexes **1** and **2**, the vanadium donor atom distances increase slightly. For example, the vanadium carbene distances expand from 2.055(3) Å to 2.070(3) Å and from 2.131(3) Å to 2.153(7) Å during the reduction to

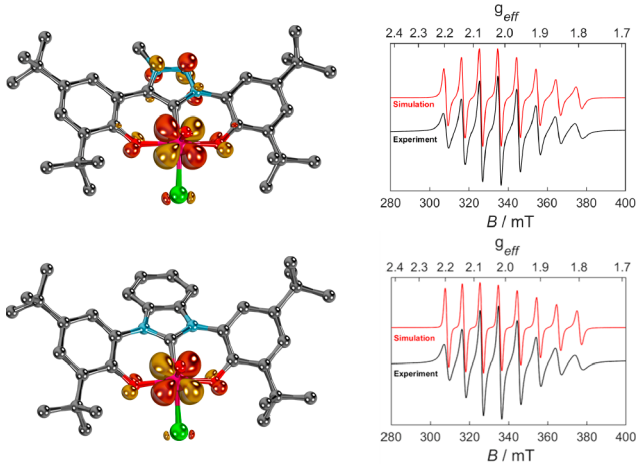

Figure 3. Compounds [**Co(Cp*)$_2$**][**1**] (top left) and [**Co(Cp*)$_2$**][**2**] (bottom left) feature unpaired electrons in the 3d(*yz*) orbitals (QROs). X-band EPR spectra of [**Co(Cp*)$_2$**][**1**] (top right) and [**Co(Cp*)$_2$**][**2**] (bottom right) of 5 mM solutions in CH_2Cl_2 at 300 K; black traces show the experimentally observed spectra and red traces the corresponding simulations. Hydrogen atoms have been omitted for clarity.

[**Co(Cp*)$_2$**][**1**] and [**Co(Cp*)$_2$**][**2**], respectively. Similarly, the phenolate distances elongate by almost 0.1 Å (compare Table S3). This is in line with the larger ionic radius of a vanadium(IV) compared to a vanadium(V) ion, which suggests the reduction is vanadium centered. The center of the redox processes was further corroborated by EPR spectroscopy (Figure 3, right). Both complexes, [**Co(Cp*)$_2$**][**1**] and [**Co(Cp*)$_2$**][**2**] show a characteristic eight-line spectrum, which is consistent with a single unpaired electron located at the metal (^{51}V, 99.75% natural abundance, I = 7/2). Values of g_{iso} = 1.9715 and g_{iso} = 1.9666 and a = [274.1915, 268.8744, 258.6040 MHz] and a = [256.8, 267.7, 261.9 MHz] for [**Co(Cp*)$_2$**][**1**] and [**Co(Cp*)$_2$**][**2**], respectively, are comparable with other vanadium(IV) complexes, for example, a four-coordinate vanadium alkylidene.[121] The electronic structure was corroborated by scalar relativistic DFT calculations at the ZORA-PBE-D3BJ/def2-TZVPP//ZORA-PBE-D3BJ/def2-SVP level of theory,[122−132] which indicate a vanadium centered SOMO (quasi-restricted orbital QRO, Figure 3, left) with only small orbital overlap with the supporting ligand.

Further evidence for the stronger donor character of the mesoionic carbene ligand **L^1** compared to the benzimidazolinylidene **L^2** can be extracted from UV−vis spectroscopy. When changing from the MIC complex **1** to the benzNHC complex **2**, the charge-transfer (CT) band located at 387 nm for **1** shifts

https://doi.org/10.1021/acs.inorgchem.1c02087
Inorg. Chem. 2021, 60, 15421−15434

Scheme 3. Salt Metathesis Reactivity of Complex 1 toward Various Chalcogen and Pnictogen-Based Nucleophiles as Well as Aryl Anion Donors

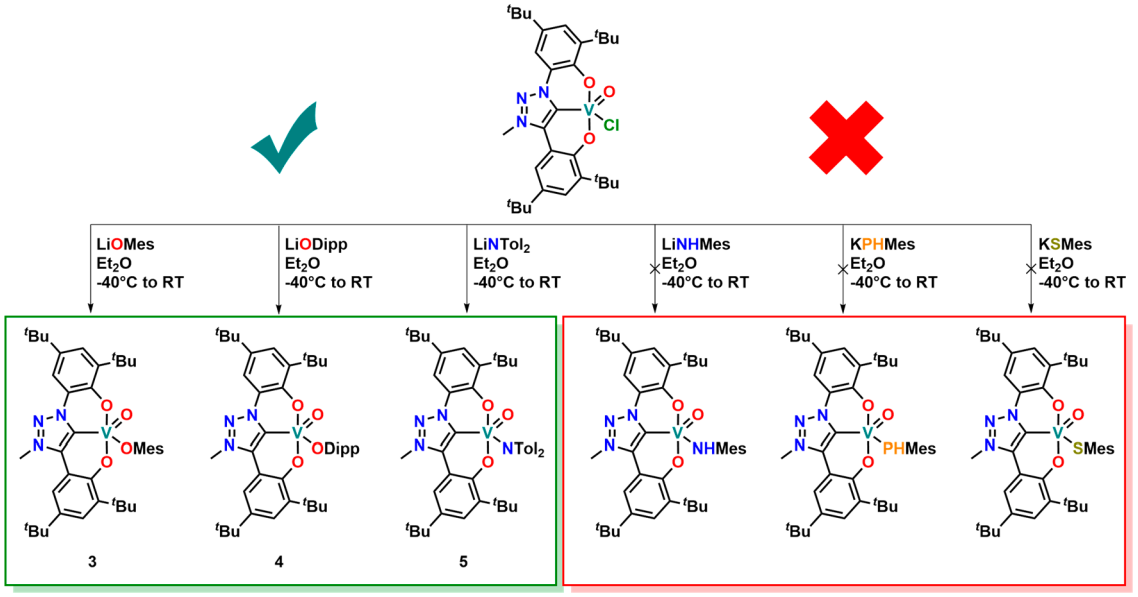

to 420 nm for **2**. Based on time-dependent DFT calculations (Figures S74−S89), we assign this band as essentially ligand-to-ligand charge transfer (LLCT) from the phenolate moieties to the NHC bridge, with only minor contribution from the metal. As the benzNHC is a stronger acceptor ligand compared to the MIC, this band is red-shifted in **2** compared to **1**.[133] The broad bands located between 500 and 800 nm in **1** and **2** are assigned to the respective ligand-to-metal charge transfers (LMCTs). This assignment is in line with their disappearance in the reduced complexes [**Co(Cp*)$_2$**][**1**] and [**Co(Cp*)$_2$**][**2**] (see Figure 4). Overall, the results from NMR, electrochemistry, and UV−vis absorption spectroscopy support the notion of MICs being stronger donors than benzNHCs in vanadium complexes.

To further explore the chemical potential of the triazolinylidene complex **1**, we turned our interest toward salt metathesis replacing the remaining chloride ligand (Scheme 3). Mixing the parent lithium salts with **1** in −40 °C cold diethyl ether, followed by recrystallization from hexane, gave the pure mesitolate (**3**), 2,6-diisopropylphenolate (**4**), and 4,4′-ditolylamide (**5**) complexes in good to moderate yields. To our surprise, the reaction with primary amides (LiNHMes), thiophenolates (KSMes), and phosphanides (KPHMes) failed to give well-defined products under the above-described conditions. Similarly, anionic alkyl or aryl donors, unrelated to their source (lithium or Grignard reagents), resulted in complicated reaction mixtures from which no defined reaction products could be isolated. The NMR spectroscopic and structural analyses (Figure 5) of the complexes **3**−**5** resemble the expected characteristics. For further information we refer to Figures S11−S25 and Tables S2 and S3 in the Supporting Information. Notably, we found that the coligand had a strong influence on the UV−vis spectroscopic features of the complexes. While the halide complex **1** was deep green (λ_{max} = 582 nm; ε = 1000 L mol^{-1} cm^{-1}), the phenolate complexes **3** and **4** are a deep purple color (λ_{max} = 534 nm; ε = 4400 L mol^{-1} cm^{-1} for complex **4**), and the amide complex **5** is dark teal (λ_{max} = 660 nm; ε = 7200 L mol^{-1} cm^{-1}, compare also Figure S68).

By further probing the versatility of complex **1**, we examined oxo-exchange reactions, with emphasis on generating vanadium imido complexes. To reach this goal, we applied

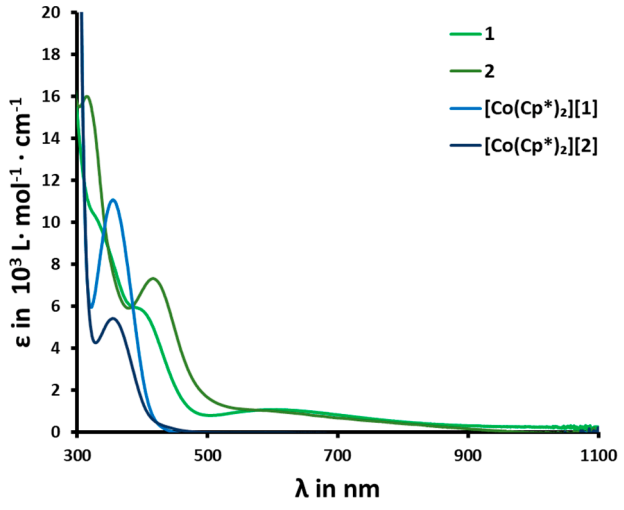

Figure 4. Stacked UV−vis spectra of the complexes **1**, **2**, [**Co(Cp*)$_2$**][**1**], and [**Co(Cp*)$_2$**][**2**] in CH_2Cl_2 at 298 K.

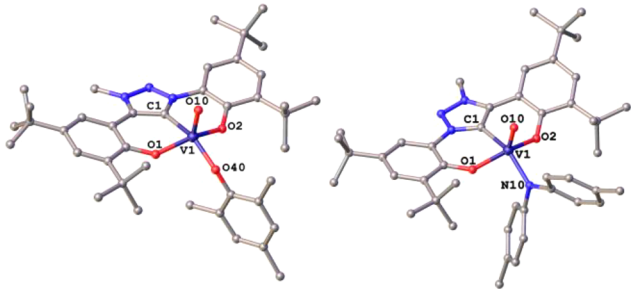

Figure 5. Molecular structures of **3** (left) and **5** (right). Hydrogen atoms and lattice solvent molecules have been omitted for clarity.

https://doi.org/10.1021/acs.inorgchem.1c02087
Inorg. Chem. 2021, 60, 15421−15434

Scheme 4. Synthesis of a Vanadium(III) Triazolinylidene Complex and Its Subsequent Conversion into Aryl and Alkyl Imido Complexes

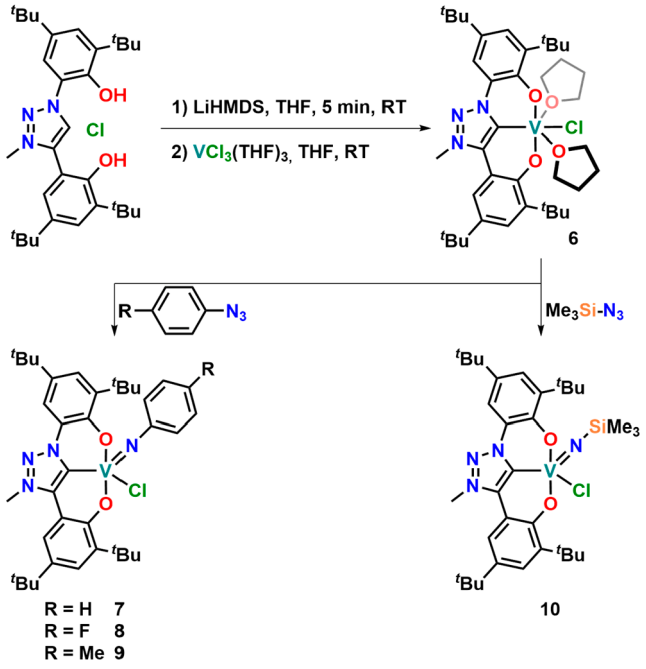

isocyanates as the imido source, liberating carbon dioxide to provide the driving force for this process. Although this strategy was successful for a plethora of vanadium imido complexes,[134,135] in the present case, even at elevated temperatures (60, 80, or 120 °C), no conversion could be observed. In one experiment (120 °C) with 3,5-bis-(trifluoromethyl)phenyl isocyanate, we observed its cyclotrimerization to yield the corresponding isocyanuric amide. It has been reported that electropositive metals, that is, Lewis acids, catalyze this process.[136−140] However, NHCs and NHOs are also known to be potent catalysts for this transformation.[141,142] As the presence of free carbenes at elevated temperatures (e.g., due to minimal thermal decomposition) cannot be fully ruled out, the catalytically active species remains unclear.

Since the direct generation of imido complexes from the oxo complexes had failed, we sought other strategies. Another versatile access to metal imido complexes is the direct reduction of organic azides by low-valent metal complexes. Thus, we initially aimed to generate a low-valent vanadium(III) complex by deoxygenating the parent vanadium(V) complex **1** with triethylphosphine. Although this strategy met with success for the deoxygenation of molybdenum(VI) benzimidazolinylidene complexes,[143,144] no useful reaction products could be isolated in the present case. Similarly, switching to other phosphines such as triphenylphosphine or trimethylphosphine turned out to be unproductive. We consequently turned our focus to installing the triazolinylidene ligand $\mathbf{L^1}$ directly on vanadium(III).[113] Although our attempts to isolate the fully deprotonated and free triazolylidene $\mathbf{Li_2[L^1]}$ have failed so far, deprotonation of $\mathbf{[H_3L^1][Cl]}$ with LiHMDS (HMDS = hexamethyldisilazide) at room temperature, followed by the immediate addition of the deprotonated triazolinylidene to $VCl_3(THF)_3$ resulted in the formation of a brown suspension. After extraction with toluene and washing of the crude solids with hexane, we isolated the desired vanadium(III) complex **6** as an orange powder in 46% yield (Scheme 4). The complex is remarkably sensitive toward air and moisture and decomposes in the glovebox at room temperature within several days even in the solid state. However, it turned out to be stable for a couple of weeks at −40 °C. The formation of the desired vanadium(III) complex was initially evident by the strong paramagnetic nature of its ^{1}H NMR, revealing an effective magnetic moment of 2.71 μ_B, which is in line with the presence of a d^2 electron configuration and is comparable to previously reported vanadium(III) complexes.[109] Despite numerous attempts and due to the high sensitivity of the complex, only low-quality crystals of the complex could be obtained from concentrated diethyl ether solutions at −40 °C. In any case, the connectivity of the molecule was unambiguously determined, confirming the vanadium(III) oxidation state (Figure 6, left). In addition to the triazolinylidene and the halide ligands, complex **6** was found to further hold two tetrahydrofuran donors, creating an octahedral coordination environment around the vanadium center. As expected for an $S = 1$ spin system, the EPR spectrum at room temperature did not reveal any observable signals (Figure S90).[121,145] Computational investigation revealed both SOMOs to be vanadium centered (Figure 7) with only small orbital overlap with the supporting ligand. Accordingly, and in agreement with the experiment, these calculations indicate an adiabatic singlet−triplet gap of $\Delta E = -47$ kJ mol^{-1} in favor of the triplet state. Note that the prediction of two SOMOs is consistent with two irreversible waves of **6** observed in the cyclic voltammogram at 0.09 and 1.03 V vs Fc/Fc$^+$ in acetonitrile (Figure S73).

Having the vanadium(III) complex **6** in hand, we turned back our interest to the generation of vanadium(V) imido complexes following an azide reduction strategy. As envisioned, complex **6** reacts smoothly with organic azides such as phenyl, 4-fluorophenyl, or 4-methylphenyl azide to

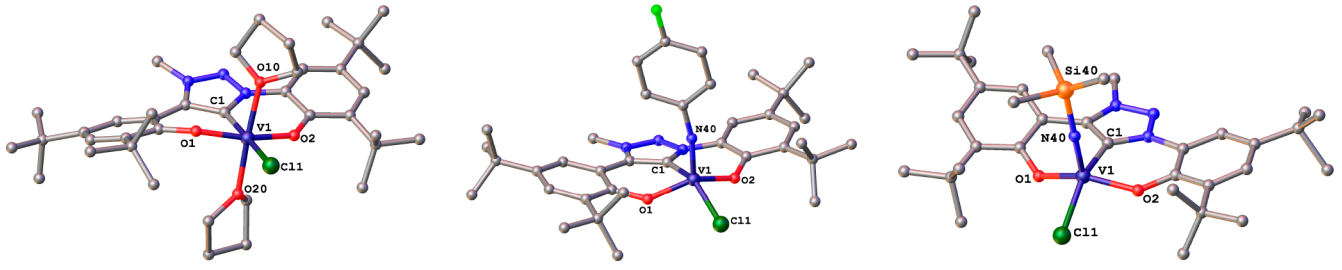

Figure 6. Molecular structures of the vanadium(III) complex **6** and the imido complexes **8** and **10** (from left to right). Hydrogen atoms and lattice solvent molecules have been omitted for clarity.

https://doi.org/10.1021/acs.inorgchem.1c02087
Inorg. Chem. 2021, 60, 15421−15434

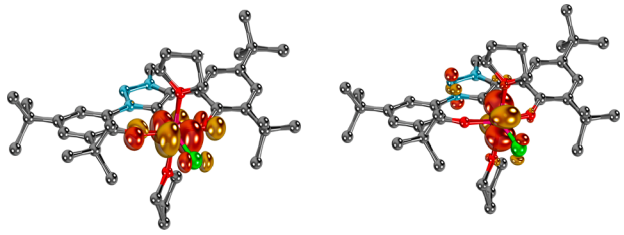

Figure 7. Compound **6** features unpaired electrons in the 3d(xz) and 3d(xy) orbitals (QROs). Hydrogen atoms have been omitted for clarity.

form the corresponding vanadium(V) imido complexes **7**, **8**, and **9**. Upon addition of the azides to benzene solutions of complex **6** and heating the samples to 60 °C, gas evolution was observed, and the reddish-brown solution gradually changed to deep green. The reaction could be followed by ^{1}H NMR spectroscopy, revealing the clean conversion to the desired complexes, which can be isolated by evaporation of benzene and washing the green powders with hexane in yields of 46−100% (Scheme 4). While the proton resonances of the complexes show the expected characteristics, the ^{13}C carbene resonance could not be observed again due to the large quadrupole moment of the ^{51}V nucleus. Similar problems occurred during our attempts to observe the imido nitrogen atom using ^{1}H−^{15}N HMBC NMR experiments. However, in the ^{51}V NMR, the complexes show resonances at −398.0, −396.8, and −378.2 ppm for **7**, **8**, and to **9** respectively (Figures S32, S38, and S43). To unambiguously prove the structural identity, X-ray quality crystals of complex **8** were grown from concentrated diethyl ether solution (Figure 6, middle). The complex crystallizes in the monoclinic space group $P2_1/n$ with one molecule in the asymmetric unit. The vanadium center is penta-coordinate by the ligand, the imido nitrogen atom, and a chlorido ligand in a slightly distorted square pyramidal coordination environment (τ_5 = 0.10). The V1−N40 distance was found to be 1.644(2) Å and is comparable to previously reported vanadium(V) imido complexes. The metal carbene distance V1−C1 was found to be 2.048(2) Å, which compares well to complex **1**. The structural parameters of the ligand are similar to complex **1** and can be found in the Supporting Information in Tables S2 and S3.

In sight of the swift reduction of organic azides, we next turned our interest toward the use of "inorganic" azides, which we envisioned to form vanadium nitrido complexes. These complexes are relevant intermediates in the context of dinitrogen activation and valorization. Indeed, reacting complex **6** with 1 equiv of TMS-N_3 resulted in the clean conversion to diamagnetic **10** at 60 °C (Scheme 4). After workup, the ^{1}H NMR spectrum of the new complex shows a single resonance at −0.31 ppm integrating nine protons, which is indicative of the remainder of the TMS group on the nitrogen atom and thus the formation of a TMS-imido complex. Indeed, Mindiola and co-workers recently reported that the cleavage of a TMS group from a TMS-imido ligand to form the corresponding nitride complex is not trivial also for other group 5 metals, for example, tantalum(V).[146] The ^{51}V-NMR shows a single resonance at −473.5 ppm (Figure S48) which is high-field shifted compared to the aryl-imido complexes **7**−**9**. However, this high-field shift can be attributed to the stronger donor character of alkyl/TMS imido versus and aryl imido ligands. Unfortunately, due to the quadrupolar moment of vanadium, the detection of both the imido nitrogen atom as well as of the silicon atom using ^{29}Si NMR spectroscopy failed. Nevertheless, X-ray quality crystals of complex **10** could be grown from slow evaporation of a concentrated diethyl ether solution at room temperature (Figure 6, right). The structural analysis confirmed the formation of the terminal imido instead of the desired nitrido complex. The structural properties of complex **10** resemble those of complex **8** and are given in the Supporting Information in Tables S2 and S3. In contrast to previous reports,[147] applying sodium azide as a nitrogen/azide source resulted in complicated (paramagnetic) mixtures, from which no defined products could be isolated.

CONCLUSIONS

We have extended the use of mesoionic carbenes with an early transition metal, vanadium. Using combined spectroscopic, electrochemical, and computational methods, we have shown that mesoionic carbenes are stronger donors than classical NHCs in early transition-metal chemistry as well. The high-valent oxo-vanadium(V) complexes are of moderate use for salt metathesis, reacting cleanly only with phenolates and secondary amides. Remarkably, the mesoionic carbene ligand supports vanadium in three oxidations states (III/IV/V). This is a rare report of a structurally characterized low-valent vanadium(III) complex supported by an NHC ligand[112−114,148] and the first of a mesoionic carbene stabilizing a low-valent early transition metal. Complex **6** is a powerful two-electron reductant and forms the corresponding high-valent vanadium(V) imido complexes with azides. In recent years, NHC-imido vanadium complexes have attracted a large interest as polymerization catalysts as well as in nitrene transfer reactions.[149] Following the concept of extreme π-loading effects[150] and given the numerous examples of superior activity of MIC based catalysts over their NHC congeners,[151] we believe that our findings will create further interest in the use of mesoionic carbenes in early transition-metal-mediated reactions. Additionally, the redox-active nature of the phenolate tethers will also be of large interest in other catalytic reactions as well as small molecule activation.

EXPERIMENTAL SECTION

General Remarks. If not otherwise mentioned, all transformations were carried out in an argon-filled glovebox under inert conditions. Solvents were dried by an MBraun SPS system and stored over activated molecular sieves (3 Å) for at least 1 day. C_6D_6 was dried over sodium/benzophenone and $CDCl_3$ and CD_2Cl_2 over calcium hydride, followed by vacuum transfer and three freeze−pump−thaw cycles. The proligand [$\mathbf{H_3L^1}$][**Cl**] was synthesized following a literature known procedure.[44] LiOMes, LiN(Tol)$_2$, and LiNHMes were obtained by deprotonating the corresponding phenol or aniline in pentane using *n*-BuLi and filtering off the products. In a similar way, KSMes and KPHMes were obtained by deprotonating the corresponding thiophenol and primary phosphine using KHMDS in toluene.[152] 4-Methylphenyl azide[153] and 4-fluorophenyl azide[154] were synthesized following previously reported methods using *tert*-butyl nitrite and trimethylsilyl azide in acetonitrile. Decamethylcobaltocene, triethylphosphine, trimethylsilyl azide, sodium azide, and VO(O^iPr)$_3$ were used as received by commercial suppliers. NMR spectra were collected at ambient temperature on a Bruker AV-300, Ascent 400, AV-500, or an Ascent 700 spectrometer. ^{1}H and ^{13}C NMR chemical shifts (δ) are reported in ppm and were calibrated to residual solvent peaks. ^{51}V NMR chemical shifts have been calibrated to $VOCl_3$ in $CDCl_3$ as an external standard. It needs to be mentioned

https://doi.org/10.1021/acs.inorgchem.1c02087
Inorg. Chem. 2021, 60, 15421−15434

at this point that ^{51}V NMR is extremely sensitive and minor impurities (0.5% <) can still be observed, even though the remaining characterization data appear to be clean. This explains the minor impurities observed in the ^{51}V NMR spectra of the complexes **1**, **4**, **5**, **7**, **8**, **9** and **10**. Elemental analysis was performed using an Elementar vario microcube instrument. IR spectra were collected using a Bruker Alpha IR spectrometer. Cyclic voltammetry was recorded using a BioLogic potentiostat and a three-electrode array (working electrode: glassy carbon, counter electrode: platinum, reference electrode: silver). EPR spectra were recorded from 5 mM solutions at 300 K using a Bruker Magnettech 5000 EPR spectrometer (microwave frequency, 9.46 GHz; microwave power, 5 mW; modulation amplitude, 0.5 mT). CW spectra were processed using MATLAB and EasySpin software package (see Supporting Information for details).[155]

Synthetic Procedures. *General Procedure for the Synthesis of **1** and **2**.* The synthesis of the complexes was adapted from the literature.[54] If not otherwise stated, the corresponding azolium salt (1 equiv, 1 mmol) was mixed with [VO(O^{i}Pr)] (1 or 1.2 equiv) in THF (30 mL) and stirred at room temperature for 2 days. The solvent was evaporated, and the resulting solids were suspended in hexane (20 mL) and stirred for 1 h at room temperature. The resulting suspension was filtered, and the solids were washed with minimal amounts of pentane (10 mL) and dried on the frit inside the glovebox to give the desired vanadium(V) complexes in yields of 78% and higher.

*[VOCl(L^1)] (**1**).* From [**H$_3$L^1**][**Cl**] (1 equiv., 1 mmol, 528 mg) and VO(O^{i}Pr)$_3$ (1 equiv., 1 mmol, 244 mg). Yield: 85% (0.85 mmol, 503 mg). ^{1}H NMR (C_6D_6, 298 K, 700 MHz, in ppm): δ = 8.06 (d, J = 2.4 Hz, 1H, Aryl-*H*), 7.75 (d, J = 2.4 Hz, 1H, Aryl-*H*), 7.73 (d, J = 2.4 Hz, 1H, Aryl-*H*), 7.10 (d, J = 2.4 Hz, 1H, Aryl-*H*). 3.17 (s, 3H, N-CH_3), 1.87 (s. 18H, C(CH_3)$_3$), 1.38 (s. 9H, C(CH_3)$_3$). 1.35 (s. 9H, C(CH_3)$_3$); ^{13}C{^{1}H} NMR(C_6D_6, 298 K, 176 MHz, in ppm): δ = 162.5 (Aryl-*C*-OH), 1.55 (Aryl-*C*-OH), 143.7 (Aryl-*C*), 142.8 (Aryl-*C*), 141.6 (Aryl-*C*), 140.7 (Aryl-*C*), 140.1 (Aryl-*C*), 127.1 (Aryl-CH), 126.3 (Aryl-CH), 124.3 (Aryl-*C*), 118.6 (Aryl-CH), 113.6 (Aryl-CH), 113.2 (Aryl-*C*), 39.7 (N-CH$_3$), 36.9 (*C*(CH$_3$)$_3$), 36.7 (*C*(CH$_3$)$_3$), 35.4 (*C*(CH$_3$)$_3$), 35.2 (*C*(CH$_3$)$_3$), 32.2 (*C*(CH$_3$)$_3$), 32.1 (*C*(CH$_3$)$_3$), 30.8 (C(*C*H$_3$)$_3$), 30.7 (C(*C*H$_3$)$_3$); ^{51}V NMR(C_6D_6, 298 K, 184 MHz, in ppm): δ = −533 (s). Elemental analysis (%) calcd for $C_{31}H_{43}N_3O_3VCl$: C, 62.89; H, 7.32; N, 7.10; found C, 62.53; H, 7.12; N, 6.86.

*[VOCl(L^2)] (**2**).* From [**H$_3$L^2**][**Cl**] (1 equiv., 1 mmol, 563 mg) and VO(O^{i}Pr)$_3$ (1.2 equiv., 1.2 mmol, 293 mg). Yield: 91% (0.91 mmol, 571 mg). ^{1}H NMR (C_6D_6, 298 K, 700 MHz, in ppm): δ = 7.81 (m, 2H Aryl-*H*), 7.67 (d, J = 2.4 Hz, 2H, Aryl-*H*), 7.65 (d, J = 2.4 Hz, 2H, Aryl-*H*), 7.00 (m, 2H, Aryl-*H*), 1.87 (s, 18H, C(CH_3)$_3$), 1.36 (s, 18H, C(CH_3)$_3$); ^{13}C{^{1}H} NMR(C_6D_6, 298 K, 176 MHz, in ppm): δ = 155.4 (Aryl-*C*-OH), 143.3 (Aryl-*C*), 139.9 (Aryl-*C*), 133.2 (Aryl-*C*), 128.6 (Aryl-*C*), 125.6 (Aryl-CH), 123.6 (Aryl-*C*), 123.4 (Aryl-CH), 115.4 (Aryl-CH), 114.4 (Aryl-CH), 36.2 (*C*(CH$_3$)$_3$), 34.9 (*C*(CH$_3$)$_3$), 31.7 (C(*C*H$_3$)$_3$), 30.3 (C(*C*H$_3$)$_3$); ^{51}V NMR (C_6D_6, 298 K, 184 MHz, in ppm): δ = −503 (s). Elemental analysis (%) calcd for $C_{35}H_{44}N_2O_3VCl$: C, 67.03; H, 7.07; N, 4.47; found C, 66.94; H, 7.12; N, 4.21.

*General Procedure for **[Co(Cp*)$_2$][1]** and **[Co(Cp*)$_2$][2]**.* The parent vanadium(V) complexes **1** or **2** (1 equiv.) were dissolved in THF and stirred for 10 min at room temperature. A solution of decamethylcobaltocene (1 equiv.) in THF was added, and the reaction mixtures were stirred for 5 h at room temperature.

[Co(Cp)$_2$][VOCl(L^1)] (**[Co(Cp*)$_2$][1]**).* From complex **1** (1 equiv., 0.25 mmol, 148 mg) and Co(Cp*)$_2$ (1 equiv., 0.25 mmol, 83 mg). After 5 h the reaction was filtered, and the solvent was evaporated. The greenish-gray residue was dissolved in CH_2Cl_2 and filtered again and concentrated to 1 mL. Hexane was added until the solution became turbid. One drop of dichloromethane was added to redissolve all solids, and the mixture was left to stand in an openly capped vial inside the glovebox for 2 days to let the dichloromethane evaporate. This formed large green blocks of [**Co(Cp*)$_2$**][**1**]. Yield: 76% (0.19 mmol, 175.1 mg). Elemental analysis (%) calcd for $C_{51}H_{74}N_3O_3VCoCl$: C, 66.48; H, 7.99; N, 4.56; found C, 66.75; H, 7.66; N, 4.28, μ_{eff} = 1.74 μB.

[Co(Cp)$_2$][VOCl(L^2)] (**[Co(Cp*)$_2$][2]**).* From complex **2** (1 equiv., 0.25 mmol, 157 mg) and Co(Cp*)$_2$ (1 equiv., 0.25 mmol, 83 mg). After 5 h, the green suspension was filtered, and the green solids were washed with another 5 mL of THF and 5 mL of pentane. The green solids were then dissolved in 5 mL of dichloromethane, and the solution was concentrated to 1 mL. Hexane was added until the solution became turbid. One drop of dichloromethane was added to redissolve all solids, and the mixture was left to stand in an openly capped vial for 2 days inside the glovebox to let the dichloromethane evaporate. This formed large green blocks of [**Co(Cp*)$_2$**][**1**]. Yield: 69% (0.172 mmol, 165 mg). Elemental analysis (%) calcd for $C_{55}H_{74}N_2O_3VCoCl$: C, 69.06; H, 7.80; N, 2.93; found C, 68.37; H, 7.54; N, 2.82, μ_{eff} = 1.68 μB.

General Procedure for the Salt Metathesis Reactions. In a 20 mL scintillation vial, vanadium complex **1** was dissolved in 5 mL Et$_2$O and cooled to −40 °C. In a separate vial, the corresponding lithium salt (phenolate or amide) was dissolved/suspended in 2 mL Et$_2$O and cooled to −40 °C as well. This solution was then added dropwise at −40 °C to the solution of the vanadium complex and slowly warmed to room temperature overnight while stirring. The deeply colored solutions are filtered to remove any lithium chloride formed during the reaction, and the solvent was evaporated under high vacuum. The colored residues were then dissolved in hexane, filtered again, and concentrated to approximately 0.5 mL. Storing these solutions at −40 °C resulted in the formation of the corresponding complexes in moderate to good yields overnight.

*[VO(OMes)(L^1)] (**3**).* Following the general procedure, LiOMes (1 equiv., 0.1 mmol, 14 mg) was added to **1** (1 equiv., 0.1 mmol, 59 mg). Dark purple solid. Yield: 98% (68 mg, 0.098 mmol). ^{1}H NMR (C_6D_6, 298 K, 400 MHz, in ppm) δ 8.17 (d, J = 2.4 Hz, 1H, Aryl-*H*), 7.73 (d, J = 2.4 Hz, 1H, Aryl-*H*), 7.69 (d, J = 2.5 Hz, 1H, Aryl-*H*), 7.13 (d, J = 2.3 Hz, 1H, Aryl-*H*), 6.92 (s, 1H, Mesityl-*H*), 6.71 (s, 1H, Mesityl-*H*), 3.07 (s, 3H, N-CH_3), 3.02 (s, br, 3H, C-CH_3), 2.32 (s, br, 3H, C-CH_3), 2.20 (s, 3H, C-CH_3), 1.69 (s, 9H, C-(CH_3)$_3$), 1.62 (s, 9H, C-(CH_3)$_3$), 1.41 (s, 9H, C-(CH_3)$_3$), 1.38 (s, 9H, C-(CH_3)$_3$). ^{13}C NMR (C_6D_6, 298 K, 101 MHz, in ppm) δ 162.02 (Aryl-*C*-OH), 155.16 (Aryl-*C*-OH), 141.59 (Aryl-*C*), 141.39 (Aryl-*C*), 140.49 (Aryl-*C*), 139.86 (Aryl-*C*), 132.23 (Aryl-*C*), 129.51 (Aryl-*C*), 128.99 (Aryl-CH), 128.87 (Aryl-CH), 126.18 (Aryl-CH), 125.53 (Aryl-CH), 125.27 (Aryl-CH), 122.96 (Aryl-CH), 118.52 (Aryl-CH), 113.82 (Aryl-CH), 113.68 (Aryl-CH), 38.82 (N-CH$_3$), 36.21 (*C*(CH$_3$)$_3$), 36.11 (*C*(CH$_3$)$_3$), 34.81 (*C*(CH$_3$)$_3$), 34.66 (*C*(CH$_3$)$_3$), 31.86 (C(*C*H$_3$)$_3$), 31.77 (C(*C*H$_3$)$_3$), 30.04 (C(*C*H$_3$)$_3$), 29.90 (C(*C*H$_3$)$_3$), 21.13 (C-CH$_3$), 18.49 (C-CH$_3$), 17.99 (C-CH$_3$). ^{51}V NMR (C_6D_6, 298 K, 79 MHz, in ppm) δ −566.66. Elemental analysis (%) calcd for $C_{40}H_{54}N_3O_4V_1$: C, 69.44; H, 7.87; N, 6.07; found C, 69.81; H, 8.16; N, 5.91.

*[VO(ODipp)(L^1)] (**4**).* Following the general procedure, LiODipp (1 equiv., 0.05 mmol, 10 mg) was added to **1** (1 equiv., 0.05 mmol, 30 mg). Dark purple solid. Yield: 96% (35 mg, 0.048 mmol). ^{1}H NMR (C_6D_6, 298 K,700 MHz, in ppm) δ 8.26 (d, 1H, J = 2.3 Hz, Aryl-*H*), 7.84 (d, 1H, J = 2.0 Hz, Aryl-*H*), 7.79 (d, 1H, J = 2.4 Hz, Aryl-*H*), 7.40 (dd, 1H, J = 7.6 Hz, J = 1.6 Hz, Aryl-*H*), 7.22 (d, 1H, J = 2.3 Hz, Aryl-*H*), 7.15 (dd, 1H, J = 7.8 Hz, J = 2.0 Hz, Aryl-*H*), 7.00 (t, 1H, J = 7.6 Hz, Aryl-*H*), 4.95 (m, 1H, C*H*(CH$_3$)$_2$), 3.55 (m, 1H, C*H*(CH$_3$)$_2$), 3.16 (s, 3H, NCH_3), 1.83 (d, 6H, J = 6.8 Hz, CHCH_3), 1.82 (s, 9H, CCH_3), 1.57 (d, 6H, J = 6.9 Hz, CHCH_3), 1.72 (s, 9H, CCH_3), 1.48 (s, 9H, CCH_3), 1.47 (s, 9H, CCH_3), 1.22 (d, 6H, J = 7.0 Hz, CHCH_3), 1.22 (d, 6H, J = 6.8 Hz, CHCH_3). ^{13}C NMR (C_6D_6, 175 MHz, in ppm): δ 167.27 (*C*-OH), 162.52 (*C*-OH), 155.68, 142.07, 141.80, 141.67, 140.99, 140.38, 140.11, 139.21, 126.63, 126.00, 125.53, 124.02, 123.53, 123.46, 118.88, 114.14, 114.07, 39.20 (NCH_3), 36.56 (*C*CH$_3$), 36.51 (*C*CH$_3$), 35.12 (*C*CH$_3$), 34.99 (*C*CH$_3$), 32.16 (*C*CH$_3$), 32.05 (*C*CH$_3$), 30.59 (*C*CH$_3$), 30.38 (-*C*CH$_3$), 28.58 (CHCH$_3$), 28.55 (CHCH$_3$), 24.57 (CHCH$_3$), 24.40 (CHCH$_3$), 24.06 (CHCH$_3$), 23.37 (CHCH$_3$). Elemental analysis (%) calcd for $C_{43}H_{60}N_3O_4V_1$: C, 70.34; H, 8.24; N, 5.73; found C, 69.04; H, 8.21; N, 5.68. The low carbon value results from

https://doi.org/10.1021/acs.inorgchem.1c02087
Inorg. Chem. 2021, 60, 15421−15434

potential carbide formation, which is a common problem for early transition metals.

*[VO(NTol$_2$)(L^1)] (**5**).* Following the general procedure, LiN(Tol)$_2$ (1 equiv., 0.05 mmol, 10 mg) was added to **1** (1 equiv., 0.05 mmol, 30 mg). Dark blue solid. Yield: 56% (27 mg, 0.028 mmol). ^{1}H NMR (C_6D_6, 298 K, 700 MHz, in ppm): δ 8.19 (d, J = 2.5 Hz, 1H, Aryl-*H*), 8.14 (d, J = 8.3 Hz, 2H, Aryl-*H*), 7.17 (s, 1H, Aryl-*H*), 7.16 (d, J = 8.3 Hz, 2H, Aryl-*H*), 7.13 (d, J = 8.6 Hz, 2H, Aryl-*H*), 7.11 (d, J = 2.3 Hz, 1H, Aryl-*H*), 6.83−6.80 (m, 2H, Aryl-*H*), 3.07 (s, 3H, NCH_3), 2.23 (s, 3H, CH_3), 1.88 (s, 3H, CH_3), 1.70 (s, 18H, CC*H*3), 1.41 (s, 9H, CC*H*3), 1.39 (s, 9H, CC*H*3). ^{13}C NMR (C_6D_6, 298 K,175 MHz, in ppm): δ 162.48 (*C*-OH), 155.51 (*C*-OH), 154.80, 151.36, 142.82, 141.70, 140.29, 140.11, 139.00, 136.01, 12961, 129.48, 128.42, 125.88, 125.86, 125.15, 122.82, 121.44, 118.80, 113.96, 38.65 (NCH_3), 36.38 (CCH_3), 36.25 (CCH_3), 34.70 (CCH_3), 34.54 (CCH_3), 31.90 (CCH_3), 31.81 (CCH_3), 30.59 (C*C*H$_3$), 30.50 (CCH_3), 20.89 (CH_3), 20.66 (CH_3). Elemental analysis (%) calcd for $C_{45}H_{57}N_4O_3V$: C, 71.79; H, 7.63; N, 7.44; found C, 71.44; H, 7.28; N, 7.16.

*[VCl(L^1)(THF)$_2$] (**6**).* In a 20 mL scintillation vial, triazolium proligand [**H$_3$L^1**][**Cl**] (1 equiv., 1.50 mmol, 792 mg) was dissolved in 5 mL THF. To the stirring, bright yellow solution, a THF solution of lithium hexamethyldisilazide (3.3 equiv., 4.95 mmol, 828 mg) was added dropwise over a period of 10 min. After 30 min at ambient temperature, a suspension of VCl$_3$(THF)$_3$ (1 equiv., 1.50 mmol, 560 mg) was added at once. The mixture turned dark red/brown after the addition. After 15 h the mixture was filtered, the solvent was removed by evaporation. The dark brown residue was redissolved in toluene, and precipitated lithium chloride was filtered off. Toluene was removed under reduced pressure, and the residue was washed several times with a small amount hexane to give **6** as an orange-brown powder (496 mg, 46%). μ_{eff} (Evans method, C_6D_6) = 2.71 μ_B. Elemental analysis (%) calcd for $C_{35}H_{51}N_3O_3V_1$·LiCl: C, 60.87; H, 7.44; N, 6.08; found C, 61.00; H, 7.13; N 6.04.

General Procedure for Imido Complexes. In a 10 mL J. Young Schlenk flask, vanadium(III) complex **6** (1.0 equiv., 0.10 mmol, 72 mg) was dissolved in 5 mL of benzene. The corresponding azide was added to the solution, and the mixture was heated to 60 °C. After 24 h, the solvent was lyophilized. Residues were washed several times with hexane to afford clean product. X-ray quality crystals were grown from concentrated diethyl ether solution at ambient temperature.

*[V(N-Ph)Cl(L^1)] (**7**).* From azidobenzene (1.2 equiv., 0.12 mmol, 14 mg). Dark green solid. Yield: 100% (67 mg, 0.10 mmol). ^{1}H NMR (C_6D_6, 298 K, 400 MHz, in ppm) δ 8.18 (d, *J* = 2.4 Hz, 1H, Aryl-*H*), 7.80 (d, *J* = 2.3 Hz, 1H, Aryl-*H*), 7.78 (d, *J* = 2.4 Hz, 1H, Aryl-*H*), 7.18 (s, 1H, Aryl-*H*), 6.68−6.61 (m, 2H, Phenyl-*H*), 6.38 (dd, *J* = 8.5, 7.0 Hz, 2H, Phenyl-*H*), 6.31−6.25 (m, 1H, Phenyl-*H*), 3.16 (s, 3H, NCH_3), 1.99 (s, 9H, C(CH_3)$_3$), 1.97 (s, 9H, C(CH_3)$_3$), 1.38 (s, 9H, C(CH_3)$_3$), 1.35 (s, 9H, C(CH_3)$_3$). ^{13}C NMR (C_6D_6, 298 K, 101 MHz, in ppm) δ 142.22 (Aryl-*C*), 141.35 (Aryl-*C*), 140.13 (Aryl-*C*), 127.39 (Aryl-CH), 127.23 (Aryl-CH), 126.03 (Aryl-CH), 125.37 (Aryl-CH), 124.83 (Aryl-CH), 123.74 (Aryl-CH), 118.24 (Aryl-CH), 113.32 (Aryl-CH), 112.53 (Aryl-CH), 38.69 (N(CH$_3$)), 36.56 (C(CH$_3$)$_3$), 36.44 (C(CH$_3$)$_3$), 34.87 (C(CH$_3$)$_3$), 34.71 (C(CH$_3$)$_3$), 31.82 (C(CH$_3$)$_3$), 31.74 (C(CH$_3$)$_3$), 30.26 (C(CH$_3$)$_3$), 30.20 (C(CH$_3$)$_3$). ^{51}V NMR (C_6D_6, 298 K, 79 MHz, in ppm) δ −397.98. Elemental analysis (%) calcd for $C_{37}H_{48}N_4O_2V_1Cl_1$·$C_6H_6$: C, 69.30; H, 7.30; N, 7.52; found C, 69.18; H, 7.51; N 6.94.

*[V(N-4-F-phenyl))Cl(L^1)] (**8**).* From 1-azido-4-fluorobenzene (1.1 equiv., 0.11 mmol, 15 mg). Dark green solid. Yield: 83% (57 mg, 0.083 mmol). ^{1}H NMR (C_6D_6, 298 K, 400 MHz, in ppm) δ 8.18 (d, *J* = 2.4 Hz, 1H, Aryl-*H*), 7.80 (d, *J* = 2.3 Hz, 1H, Aryl-*H*), 7.78 (d, *J* = 2.5 Hz, 1H, Aryl-*H*), 7.18 (d, *J* = 2.4 Hz, 1H, Aryl-*H*), 6.46 (dd, *J* = 9.0, 5.1 Hz, 2H, Aryl-*H*), 5.94 (t, *J* = 8.8 Hz, 2H, Aryl-*H*), 3.15 (s, 3H, NCH_3), 1.98 (s, 9H, C(CH_3)$_3$), 1.97 (s, 9H, C(CH_3)$_3$), 1.37 (s, 9H, C(CH_3)$_3$), 1.34 (s, 9H, C(CH_3)$_3$). ^{13}C NMR (C_6D_6, 298 K, 101 MHz, in ppm) δ 142.36 (Aryl-*C*), 141.47 (Aryl-*C*), 126.09 (Aryl-CH), 125.44 (Aryl-CH), 123.70 (Aryl-CH), 118.22 (Aryl-CH), 115.06 (Aryl-CH), 114.83 (Aryl-CH), 113.31 (Aryl-CH), 38.65 (NCH$_3$), 36.56 (C(CH$_3$)$_3$), 36.43 (C(CH$_3$)$_3$), 31.81 (C(CH$_3$)$_3$), 31.73 (C(CH$_3$)$_3$), 30.23 (C(CH$_3$)$_3$), 30.17 (C(CH$_3$)$_3$). ^{19}F NMR (C_6D_6, 298 K, 376 MHz, in ppm) δ −109.57. ^{51}V NMR (C_6D_6, 298 K, 79 MHz, in ppm) δ −396.83. Elemental analysis (%) calcd for $C_{37}H_{47}N_4O_2F_1V_1Cl_1$·0.5 C_6H_6: C, 66.34; H, 6.96; N, 7.74; found C, 63.15; H, 6.80; N 7.39. The low carbon value results from potential carbide formation, which is a common problem for early transition metals.

*[V(N-4-Me-phenyl))Cl(L^1)] (**9**).* From 1-azido-4-methylbenzene (1.1 equiv., 0.11 mmol, 15 mg). Dark green solid. Yield: 46% (31 mg, 0.046 mmol). ^{1}H NMR (C_6D_6, 298 K, 400 MHz, in ppm) δ 8.18 (d, *J* = 2.4 Hz, 1H, Aryl-*H*), 7.80 (d, *J* = 2.3 Hz, 1H, Aryl-*H*), 7.78 (d, *J* = 2.5 Hz, 1H, Aryl-*H*), 7.18 (d, *J* = 2.3 Hz, 1H, Aryl-*H*), 6.59 (d, *J* = 8.4 Hz, 2H, Aryl-*H*), 6.19−6.16 (m, 2H, Aryl-*H*), 3.16 (s, 3H, NCH_3), 2.00 (s, 9H, C(CH_3)$_3$), 1.99 (s, 9H, C(CH_3)$_3$), 1.62 (s, 3H, CCH_3), 1.38 (s, 9H, C(CH_3)$_3$), 1.36 (s, 9H, C(CH_3)$_3$). ^{13}C NMR (C_6D_6, 298 K, 101 MHz, in ppm) δ 142.07 (Aryl-*C*), 141.18 (Aryl-*C*), 137.54 (Aryl-*C*), 128.62 (Aryl-CH), 125.97 (Aryl-CH), 125.32 (Aryl-CH), 124.93 (Aryl-CH), 123.79 (Aryl-CH), 118.26 (Aryl-CH), 113.34 (Aryl-CH), 112.58 (Aryl-CH), 38.62 (NCH$_3$), 36.58 (C(CH$_3$)$_3$), 36.46 (C(CH$_3$)$_3$), 31.84 (C(CH$_3$)$_3$), 31.76 (C(CH$_3$)$_3$), 30.27 (C(CH$_3$)$_3$), 30.21 (C(CH$_3$)$_3$), 20.88 (CCH$_3$). ^{51}V NMR (C_6D_6, 298 K, 79 MHz, in ppm) δ −378.16. Due to the high sensitivity of the complex, no satisfactory elementary analysis could be obtained.

*[V(N-TMS))Cl(L^1)] (**10**).* From azidotrimethylsilane (1.1 equiv., 0.11 mmol, 13 mg). Dark greyish-green solid. Yield: 83% (55 mg, 0.083 mmol). ^{1}H NMR (C_6D_6, 298 K, 400 MHz, in ppm) δ 8.20 (d, *J* = 2.3 Hz, 1H, Aryl-*H*), 7.77 (d, *J* = 2.3 Hz, 1H, Aryl-*H*), 7.74 (d, *J* = 2.4 Hz, 1H, Aryl-*H*), 7.24 (d, *J* = 2.3 Hz, 1H, Aryl-*H*), 3.27 (s, 3H, NCH_3), 1.96 (s, 9H, C(CH_3)$_3$), 1.95 (s, 9H, C(CH_3)$_3$), 1.37 (s, 9H, C(CH_3)$_3$), 1.34 (s, 9H, C(CH_3)$_3$), −0.31 (s, 9H, Si(CH_3)$_3$). ^{13}C NMR (C_6D_6, 298 K, 101 MHz, in ppm) δ 141.73 (Aryl-*C*), 140.82 (Aryl-*C*), 126.09 (Aryl-CH), 125.37 (Aryl-CH), 117.93 (Aryl-CH), 113.11 (Aryl-CH), 112.55 (Aryl-CH), 38.77 (NCH$_3$), 36.56 (C(CH$_3$)$_3$), 36.44 (C(CH$_3$)$_3$), 34.81 (C(CH$_3$)$_3$), 34.64 (C(CH$_3$)$_3$), 31.79 (C(CH$_3$)$_3$), 31.71 (C(CH$_3$)$_3$), 30.33 (C(CH$_3$)$_3$), 30.25 (C(CH$_3$)$_3$), 0.02 (Si(CH$_3$)$_3$). ^{51}V NMR (C_6D_6, 298 K, 79 MHz, in ppm) δ −473.46. Elemental analysis (%) calcd for $C_{34}H_{52}N_4O_2Si_1V_1Cl_1$: C, 61.57; H, 7.90; N, 8.45; found C, 59.05; H, 8.00; N 8.27. The low carbon value results from potential carbide formation, which is a common problem for early transition metals.

X-ray Crystallography. Single crystals for X-ray diffraction experiments were performed at the analytical facility of the University of Paderborn or at the University of Innsbruck. All crystals were kept at 120(2) K or 153(2) K throughout data collection. Data collection was performed using either the ApexIII software package on a Bruker D8 Venture (Paderborn) or on a Bruker D8 Quest instrument (Innsbruck). Data refinement and reduction were performed using the Bruker ApexIII suite 2021. All structures were solved with SHELXT[156] and refined using the OLEX 2 software package.[157] Strongly disordered solvent molecules were been removed using the SQUEEZE operation.[158] All nonhydrogen atoms were refined anisotropically, and hydrogen atoms were included at the geometrically calculated positions and refined using a riding model. For further crystallographic details, see Tables S2 and S3 in the Supporting Information.

■ ASSOCIATED CONTENT

Supporting Information

The Supporting Information is available free of charge at https://pubs.acs.org/doi/10.1021/acs.inorgchem.1c02087.

NMR spectra, IR spectra, UV−vis spectra, crystallographic details, cyclic voltammograms and computational details (PDF)

Accession Codes

CCDC 2079467, 2079465, 2079472, 2079471, 2079474, 2079469, 2079473 and 2080686 contain the supplementary crystallographic data for this paper. These data can be obtained

https://doi.org/10.1021/acs.inorgchem.1c02087
Inorg. Chem. 2021, 60, 15421−15434

free of charge via www.ccdc.cam.ac.uk/data_request/cif, or by emailing data_request@ccdc.cam.ac.uk, or by contacting The Cambridge Crystallographic Data Centre, 12 Union Road, Cambridge CB2 1EZ, UK; fax: + 441223 336033.

AUTHOR INFORMATION

Corresponding Authors

Stephan Hohloch − *Institute of Inorganic, General and Theoretical Chemistry, University of Innsbruck, 6020 Innsbruck, Austria;* orcid.org/0000-0002-5353-0801; Email: Stephan.Hohloch@uibk.ac.at

Dominik Munz − *Fakultät NT, Inorganic Chemistry: Coordination Chemistry, Saarland University, 66123 Saarbrücken, Germany;* orcid.org/0000-0003-3412-651X; Email: Dominik.Munz@uni-saarland.de

Authors

Florian R. Neururer − *Institute of Inorganic, General and Theoretical Chemistry, University of Innsbruck, 6020 Innsbruck, Austria*

Shenyu Liu − *Faculty of Science, Department of Chemistry, University of Paderborn, 33098 Paderborn, Germany*

Daniel Leitner − *Institute of Inorganic, General and Theoretical Chemistry, University of Innsbruck, 6020 Innsbruck, Austria*

Marc Baltrun − *Faculty of Science, Department of Chemistry, University of Paderborn, 33098 Paderborn, Germany*

Katherine R. Fisher − *Department Chemie, Ludwigs-Maximilians-University Munich, 81377 Munich, Germany*

Holger Kopacka − *Institute of Inorganic, General and Theoretical Chemistry, University of Innsbruck, 6020 Innsbruck, Austria*

Klaus Wurst − *Institute of Inorganic, General and Theoretical Chemistry, University of Innsbruck, 6020 Innsbruck, Austria*

Lena J. Daumann − *Department Chemie, Ludwigs-Maximilians-University Munich, 81377 Munich, Germany*

Complete contact information is available at: https://pubs.acs.org/10.1021/acs.inorgchem.1c02087

Author Contributions

The project was designed and created by S.H. All experiments involving the synthesis of metal complexes were carried out by F.R.N. and S.L. The proligand $[\mathbf{H_3L^1}][\mathbf{Cl}]$ was synthesized by M.B. and F.R.N. EPR spectra were recorded and simulated by D.L., K.R.F., and D.J.L. X-ray diffraction analysis was performed by S.H. and K.W. ^{51}V NMRs were recorded by H.K. Computations were performed by D.M. The manuscript was written by F.R.N., D.M., and S.H. and proofread by all authors.

Notes

The authors declare no competing financial interest.

ACKNOWLEDGMENTS

We are grateful to the Daimler and Benz Foundation, the Fonds der Chemischen Industrie, the Northrhine-Westphalian Academy of Science, Humanities, and the Arts as well as the University of Paderborn and the University of Innsbruck for funding of this work. Fabian A. Watt and Prof. Dr. Jan Paradies are kindly acknowledged for helpful discussions.

REFERENCES

(1) Gründemann, S.; Kovacevic, A.; Albrecht, M.; Faller, R. J. W.; Crabtree, R. H. Abnormal binding in a carbene complex formed from an imidazolium salt and a metal hydride complex. *Chem. Commun.* **2001**, *21*, 2274−2275.

(2) Vivancos, Á.; Segarra, C.; Albrecht, M. Mesoionic and Related Less Heteroatom-Stabilized N-Heterocyclic Carbene Complexes: Synthesis, Catalysis, and Other Applications. *Chem. Rev.* **2018**, *118* (19), 9493−9586.

(3) Crabtree, R. H. Abnormal, mesoionic and remote N-heterocyclic carbene complexes. *Coord. Chem. Rev.* **2013**, *257* (3−4), 755−766.

(4) Guisado-Barrios, G.; Bouffard, J.; Donnadieu, B.; Bertrand, G. Crystalline 1H-1,2,3-triazol-5-ylidenes: new stable mesoionic carbenes (MICs). *Angew. Chem., Int. Ed.* **2010**, *49* (28), 4759−4762.

(5) Guisado-Barrios, G.; Soleilhavoup, M.; Bertrand, G. 1 H-1,2,3-Triazol-5-ylidenes: Readily Available Mesoionic Carbenes. *Acc. Chem. Res.* **2018**, *51* (12), 3236−3244.

(6) Schweinfurth, D.; Hettmanczyk, L.; Suntrup, L.; Sarkar, B. Metal Complexes of Click-Derived Triazoles and Mesoionic Carbenes: Electron Transfer, Photochemistry, Magnetic Bistability, and Catalysis. *Z. Anorg. Allg. Chem.* **2017**, *643* (9), 554−584.

(7) Donnelly, K. F.; Petronilho, A.; Albrecht, M. Application of 1,2,3-triazolylidenes as versatile NHC-type ligands: synthesis, properties, and application in catalysis and beyond. *Chem. Commun.* **2013**, *49* (12), 1145−1159.

(8) Mathew, P.; Neels, A.; Albrecht, M. 1,2,3-Triazolylidenes as versatile abnormal carbene ligands for late transition metals. *J. Am. Chem. Soc.* **2008**, *130* (41), 13534−13535.

(9) Hettmanczyk, L.; Spall, S. J. P.; Klenk, S.; van der Meer, M.; Hohloch, S.; Weinstein, J. A.; Sarkar, B. Structural, Electrochemical, and Photochemical Properties of Mono- and Digold(I) Complexes Containing Mesoionic Carbenes. *Eur. J. Inorg. Chem.* **2017**, *2017* (14), 2112−2121.

(10) Hohloch, S.; Suntrup, L.; Sarkar, B. Exploring potential cooperative effects in dicopper(i)-di-mesoionic carbene complexes: applications in click catalysis. *Inorg. Chem. Front.* **2016**, *3* (1), 67−77.

(11) Maity, R.; Verma, A.; van der Meer, M.; Hohloch, S.; Sarkar, B. Palladium Complexes Bearing Mesoionic Carbene Ligands: Applications in α-Arylation, α-Methylation and Suzuki-Miyaura Coupling Reactions. *Eur. J. Inorg. Chem.* **2016**, *2016* (1), 111−117.

(12) Rigo, M.; Hettmanczyk, L.; Heutz, F. J. L.; Hohloch, S.; Lutz, M.; Sarkar, B.; Müller, C. Phosphinines versus mesoionic carbenes: a comparison of structurally related ligands in Au(i)-catalysis. *Dalton Trans.* **2017**, *46* (1), 86−95.

(13) Suntrup, L.; Hohloch, S.; Sarkar, B. Expanding the Scope of Chelating Triazolylidenes: Mesoionic Carbenes from the 1,5-″Click″-Regioisomer and Catalytic Synthesis of Secondary Amines from Nitroarenes. *Chem. - Eur. J.* **2016**, *22* (50), 18009−18018.

(14) Hohloch, S.; Scheiffele, D.; Sarkar, B. Activating Azides and Alkynes for the Click Reaction with [Cu(a NHC) 2 I] or [Cu(a NHC) 2] + (a NHC = Triazole-Derived Abnormal Carbenes): Structural Characterization and Catalytic Properties. *Eur. J. Inorg. Chem.* **2013**, *2013* (22−23), 3956−3965.

(15) Hohloch, S.; Frey, W.; Su, C.-Y.; Sarkar, B. Abnormal carbenes derived from the 1,5-cycloaddition product between azides and alkynes: structural characterization of Pd(II) complexes and their catalytic properties. *Dalton Trans.* **2013**, *42* (32), 11355−11358.

(16) Hettmanczyk, L.; Manck, S.; Hoyer, C.; Hohloch, S.; Sarkar, B. Heterobimetallic complexes with redox-active mesoionic carbenes as metalloligands: electrochemical properties, electronic structures and catalysis. *Chem. Commun.* **2015**, *51* (54), 10949−10952.

(17) Hohloch, S.; Hettmanczyk, L.; Sarkar, B. Introducing Potential Hemilability into "Click" Triazoles and Triazolylidenes: Synthesis and Characterization of d 6 -Metal Complexes and Oxidation Catalysis. *Eur. J. Inorg. Chem.* **2014**, *2014* (20), 3164−3171.

(18) Suntrup, L.; Stein, F.; Klein, J.; Wilting, A.; Parlane, F. G. L.; Brown, C. M.; Fiedler, J.; Berlinguette, C. P.; Siewert, I.; Sarkar, B. Rhenium Complexes of Pyridyl-Mesoionic Carbenes: Photochemical

Properties and Electrocatalytic CO2 Reduction. *Inorg. Chem.* **2020**, *59* (7), 4215−4227.
(19) Bolje, A.; Hohloch, S.; van der Meer, M.; Košmrlj, J.; Sarkar, B. Ru(II), Os(II), and Ir(III) complexes with chelating pyridyl-mesoionic carbene ligands: structural characterization and applications in transfer hydrogenation catalysis. *Chem. - Eur. J.* **2015**, *21* (18), 6756−6764.
(20) Mendoza-Espinosa, D.; González-Olvera, R.; Negrón-Silva, G. E.; Angeles-Beltrán, D.; Suárez-Castillo, O. R.; Álvarez-Hernández, A.; Santillan, R. Phenoxy-Linked Mesoionic Triazol-5-ylidenes as Platforms for Multinuclear Transition Metal Complexes. *Organometallics* **2015**, *34* (18), 4529−4542.
(21) Mendoza-Espinosa, D.; Alvarez-Hernández, A.; Angeles-Beltrán, D.; Negrón-Silva, G. E.; Suárez-Castillo, O. R.; Vásquez-Pérez, J. M. Bridged N-Heterocyclic/Mesoionic (NHC/MIC) Heterodicarbenes as Ligands for Transition Metal Complexes. *Inorg. Chem.* **2017**, *56* (4), 2092−2099.
(22) van der Meer, M.; Glais, E.; Siewert, I.; Sarkar, B. Electrocatalytic Dihydrogen Production with a Robust Mesoionic Pyridylcarbene Cobalt Catalyst. *Angew. Chem., Int. Ed.* **2015**, *54* (46), 13792−13795.
(23) Klenk, S.; Rupf, S.; Suntrup, L.; van der Meer, M.; Sarkar, B. The Power of Ferrocene, Mesoionic Carbenes, and Gold: Redox-Switchable Catalysis. *Organometallics* **2017**, *36* (10), 2026−2035.
(24) Kilpin, K. J.; Paul, U. S. D.; Lee, A.-L.; Crowley, J. D. Gold(I) "click" 1,2,3-triazolylidenes: synthesis, self-assembly and catalysis. *Chem. Commun.* **2011**, *47* (1), 328−330.
(25) Flores-Jarillo, M.; Mendoza-Espinosa, D.; Salazar-Pereda, V.; González-Montiel, S. Synthesis and Catalytic Benefits of Tetranuclear Gold(I) Complexes with a C4 -Symmetric Tetratriazol-5-ylidene. *Organometallics* **2017**, *36* (21), 4305−4312.
(26) Mejuto, C.; Guisado-Barrios, G.; Gusev, D.; Peris, E. First homoleptic MIC and heteroleptic NHC-MIC coordination cages from 1,3,5-triphenylbenzene-bridged tris-MIC and tris-NHC ligands. *Chem. Commun.* **2015**, *51* (73), 13914−13917.
(27) AL-Shnani, F.; Guisado-Barrios, G.; Sainz, D.; Peris, E. Tris-triazolium Salts as Anion Receptors and as Precursors for the Preparation of Cylinder-like Coordination Cages. *Organometallics* **2019**, *38* (3), 697−701.
(28) Stubbe, J.; Neuman, N. I.; McLellan, R.; Sommer, M. G.; Nößler, M.; Beerhues, J.; Mulvey, R. E.; Sarkar, B. Isomerization Reactions in Anionic Mesoionic Carbene-Borates and Control of Properties and Reactivities in the Resulting CoII Complexes through Agostic Interactions. *Angew. Chem., Int. Ed.* **2021**, *60* (1), 499−506.
(29) Pinter, P.; Schüßlbauer, C. M.; Watt, F. A.; Dickmann, N.; Herbst-Irmer, R.; Morgenstern, B.; Grünwald, A.; Ullrich, T.; Zimmer, M.; Hohloch, S.; Guldi, D. M.; Munz, D. Bright luminescent lithium and magnesium carbene complexes. *Chem. Sci.* **2021**, *12* (21), 7401−7410.
(30) Hettmanczyk, L.; Manck, S.; Hoyer, C.; Hohloch, S.; Sarkar, B. Heterobimetallic complexes with redox-active mesoionic carbenes as metalloligands: electrochemical properties, electronic structures and catalysis. *Chem. Commun.* **2015**, *51* (54), 10949−10952.
(31) Kleinhans, G.; Chan, A. K.-W.; Leung, M.-Y.; Liles, D. C.; Fernandes, M. A.; Yam, V. W.-W.; Fernández, I.; Bezuidenhout, D. I. Synthesis and Photophysical Properties of T-Shaped Coinage-Metal Complexes. *Chem. - Eur. J.* **2020**, *26* (31), 6993−6998.
(32) Brown, D. G.; Sanguantrakun, N.; Schulze, B.; Schubert, U. S.; Berlinguette, C. P. Bis(tridentate) ruthenium-terpyridine complexes featuring microsecond excited-state lifetimes. *J. Am. Chem. Soc.* **2012**, *134* (30), 12354−12357.
(33) Schulze, B.; Friebe, C.; Jäger, M.; Görls, H.; Birckner, E.; Winter, A.; Schubert, U. S. Pt II Phosphors with Click-Derived 1,2,3-Triazole-Containing Tridentate Chelates. *Organometallics* **2018**, *37* (1), 145−155.
(34) Nair, S. S.; Bysewski, O. A.; Kupfer, S.; Wächtler, M.; Winter, A.; Schubert, U. S.; Dietzek, B. Excitation Energy-Dependent Branching Dynamics Determines Photostability of Iron(II)-Mesoionic Carbene Complexes. *Inorg. Chem.* **2021**, *60*, 9157.
(35) Chábera, P.; Liu, Y.; Prakash, O.; Thyrhaug, E.; Nahhas, A. E.; Honarfar, A.; Essén, S.; Fredin, L. A.; Harlang, T. C. B.; Kjær, K. S.; Handrup, K.; Ericson, F.; Tatsuno, H.; Morgan, K.; Schnadt, J.; Häggström, L.; Ericsson, T.; Sobkowiak, A.; Lidin, S.; Huang, P.; Styring, S.; Uhlig, J.; Bendix, J.; Lomoth, R.; Sundström, V.; Persson, P.; Wärnmark, K. A low-spin Fe(iii) complex with 100-ps ligand-to-metal charge transfer photoluminescence. *Nature* **2017**, *543* (7647), 695−699.
(36) Maulbetsch, T.; Kunz, D. Carbenaporphyrins: No Longer Missing Ligands in N-Heterocyclic Carbene Chemistry. *Angew. Chem., Int. Ed.* **2021**, *60* (4), 2007−2012.
(37) Beerhues, J.; Aberhan, H.; Streit, T.-N.; Sarkar, B. Probing Electronic Properties of Triazolylidenes through Mesoionic Selones, Triazolium Salts, and Ir-Carbonyl-Triazolylidene Complexes. *Organometallics* **2020**, *39* (24), 4557−4564.
(38) Dong, Z.; Blaskovits, T.; Fadaei-Tirani, F.; Scopelliti, R.; Sienkiewicz, A.; Corminboeuf, C.; Severin, K. Tuning the π-Accepting Properties of Mesoionic Carbenes: A Combined Computational and Experimental Study. *Chem. - Eur. J.* **2021**, *27*, 11983.
(39) Suntrup, L.; Klenk, S.; Klein, J.; Sobottka, S.; Sarkar, B. Gauging Donor/Acceptor Properties and Redox Stability of Chelating Click-Derived Triazoles and Triazolylidenes: A Case Study with Rhenium(I) Complexes. *Inorg. Chem.* **2017**, *56* (10), 5771−5783.
(40) Beerhues, J.; Neubrand, M.; Sobottka, S.; Neuman, N. I.; Aberhan, H.; Chandra, S.; Sarkar, B. Directed Design of a AuI Complex with a Reduced Mesoionic Carbene Radical Ligand: Insights from 1,2,3-Triazolylidene Selenium Adducts and Extensive Electrochemical Investigations. *Chem. - Eur. J.* **2021**, *27* (21), 6557−6568.
(41) Munz, D. Pushing Electrons—Which Carbene Ligand for Which Application? *Organometallics* **2018**, *37* (3), 275−289.
(42) Bens, T.; Boden, P.; Di Martino-Fumo, P.; Beerhues, J.; Albold, U.; Sobottka, S.; Neuman, N. I.; Gerhards, M.; Sarkar, B. Chromium(0) and Molydenum(0) Complexes with a Pyridyl-Mesoionic Carbene Ligand: Structural, (Spectro)electrochemical, Photochemical, and Theoretical Investigations. *Inorg. Chem.* **2020**, *59* (20), 15504−15513.
(43) Boden, P.; Di Martino-Fumo, P.; Bens, T.; Steiger, S.; Albold, U.; Niedner-Schatteburg, G.; Gerhards, M.; Sarkar, B. NIR-Emissive Chromium(0), Molybdenum(0), and Tungsten(0) Complexes in the Solid State at Room Temperature. *Chem. - Eur. J.* **2021**, *27*, 12959.
(44) Baltrun, M.; Watt, F. A.; Schoch, R.; Wölper, C.; Neuba, A. G.; Hohloch, S. A new bis-phenolate mesoionic carbene ligand for early transition metal chemistry. *Dalton Trans.* **2019**, *48* (39), 14611−14625.
(45) Horrer, G.; Krahfuß, M. J.; Lubitz, K.; Krummenacher, I.; Braunschweig, H.; Radius, U. N -Heterocyclic Carbene and Cyclic (Alkyl)(amino)carbene Complexes of Titanium(IV) and Titanium(III). *Eur. J. Inorg. Chem.* **2020**, *2020* (3), 281−291.
(46) Bellemin-Laponnaz, S.; Dagorne, S. Group 1 and 2 and early transition metal complexes bearing N-heterocyclic carbene ligands: coordination chemistry, reactivity, and applications. *Chem. Rev.* **2014**, *114* (18), 8747−8774.
(47) Taakili, R.; Canac, Y. NHC Core Pincer Ligands Exhibiting Two Anionic Coordinating Extremities. *Molecules* **2020**, *25* (9), 2231.
(48) Zhang, D.; Zi, G. N-heterocyclic carbene (NHC) complexes of group 4 transition metals. *Chem. Soc. Rev.* **2015**, *44* (7), 1898−1921.
(49) Romain, C.; Bellemin-Laponnaz, S.; Dagorne, S. Recent progress on NHC-stabilized early transition metal (group 3−7) complexes: Synthesis and applications. *Coord. Chem. Rev.* **2020**, *422*, 213411.
(50) Romain, C.; Miqueu, K.; Sotiropoulos, J.-M.; Bellemin-Laponnaz, S.; Dagorne, S. Non-innocent behavior of a tridentate NHC chelating ligand coordinated onto a zirconium(IV) center. *Angew. Chem., Int. Ed.* **2010**, *49* (12), 2198−2201.
(51) Romain, C.; Heinrich, B.; Laponnaz, S. B.; Dagorne, S. A robust zirconium N-heterocyclic carbene complex for the living and highly stereoselective ring-opening polymerization of rac-lactide. *Chem. Commun.* **2012**, *48* (16), 2213−2215.

https://doi.org/10.1021/acs.inorgchem.1c02087
Inorg. Chem. 2021, 60, 15421−15434

(52) Romain, C.; Choua, S.; Collin, J.-P.; Heinrich, M.; Bailly, C.; Karmazin-Brelot, L.; Bellemin-Laponnaz, S.; Dagorne, S. Redox and luminescent properties of robust and air-stable N-heterocyclic carbene group 4 metal complexes. *Inorg. Chem.* **2014**, *53* (14), 7371−7376.
(53) Romain, C.; Brelot, L.; Bellemin-Laponnaz, S.; Dagorne, S. Synthesis and Structural Characterization of a Novel Family of Titanium Complexes Bearing a Tridentate Bis-phenolate-N-heterocyclic Carbene Dianionic Ligand and Their Use in the Controlled ROP of rac -Lactide. *Organometallics* **2010**, *29* (5), 1191−1198.
(54) Bellemin-Laponnaz, S.; Welter, R.; Brelot, L.; Dagorne, S. Synthesis and structure of V(V) and Mn(III) NHC complexes supported by a tridentate bis-aryloxide-N-heterocyclic carbene ligand. *J. Organomet. Chem.* **2009**, *694* (5), 604−606.
(55) Hessevik, J.; Lalrempuia, R.; Nsiri, H.; Törnroos, K. W.; Jensen, V. R.; Le Roux, E. Sterically (un)encumbered mer-tridentate N-heterocyclic carbene complexes of titanium(iv) for the copolymerization of cyclohexene oxide with CO2. *Dalton Trans.* **2016**, *45* (37), 14734−14744.
(56) Lalrempuia, R.; Breivik, F.; Törnroos, K. W.; Le Roux, E. Coordination behavior of bis-phenolate saturated and unsaturated N-heterocyclic carbene ligands to zirconium: reactivity and activity in the copolymerization of cyclohexene oxide with CO2. *Dalton Trans.* **2017**, *46* (25), 8065−8076.
(57) Suresh, L.; Lalrempuia, R.; Ekeli, J. B.; Gillis-D'Hamers, F.; Törnroos, K. W.; Jensen, V. R.; Le Roux, E. Unsaturated and Benzannulated N-Heterocyclic Carbene Complexes of Titanium and Hafnium: Impact on Catalysts Structure and Performance in Copolymerization of Cyclohexene Oxide with CO2. *Molecules* **2020**, *25* (19), 4364.
(58) Despagnet-Ayoub, E.; Henling, L. M.; Labinger, J. A.; Bercaw, J. E. Group 4 Transition-Metal Complexes of an Aniline−Carbene−Phenol Ligand. *Organometallics* **2013**, *32* (10), 2934−2938.
(59) Despagnet-Ayoub, E.; Miqueu, K.; Sotiropoulos, J.-M.; Henling, L. M.; Day, M. W.; Labinger, J. A.; Bercaw, J. E. Unexpected rearrangements in the synthesis of an unsymmetrical tridentate dianionic N-heterocyclic carbene. *Chem. Sci.* **2013**, *4* (5), 2117.
(60) Despagnet-Ayoub, E.; Takase, M. K.; Henling, L. M.; Labinger, J. A.; Bercaw, J. E. Mechanistic Insights on the Controlled Switch from Oligomerization to Polymerization of 1-Hexene Catalyzed by an NHC-Zirconium Complex. *Organometallics* **2015**, *34* (19), 4707−4716.
(61) Weinberg, D. R.; Hazari, N.; Labinger, J. A.; Bercaw, J. E. Iridium(I) and Iridium(III) Complexes Supported by a Diphenolate Imidazolyl-Carbene Ligand. *Organometallics* **2010**, *29* (1), 89−100.
(62) Spencer, L. P.; Fryzuk, M. D. Synthesis and reactivity of zirconium and hafnium complexes incorporating chelating diamido-N-heterocyclic-carbene ligands. *J. Organomet. Chem.* **2005**, *690* (24−25), 5788−5803.
(63) Arnold, P. L.; Marr, I. A.; Zlatogorsky, S.; Bellabarba, R.; Tooze, R. P. Activation of carbon dioxide and carbon disulfide by a scandium N-heterocyclic carbene complex. *Dalton Trans.* **2014**, *43* (1), 34−37.
(64) Arnold, P. L.; Marr, I. A.; Zlatogorsky, S.; Bellabarba, R.; Tooze, R. P. Activation of carbon dioxide and carbon disulfide by a scandium N-heterocyclic carbene complex. *Dalton Trans.* **2014**, *43* (1), 34−37.
(65) Arnold, P. L.; Zlatogorsky, S.; Jones, N. A.; Carmichael, C. D.; Liddle, S. T.; Blake, A. J.; Wilson, C. Comparisons between yttrium and titanium N-heterocyclic carbene complexes in the search for early transition metal NHC backbonding interactions. *Inorg. Chem.* **2008**, *47* (19), 9042−9049.
(66) Mungur, S. A.; Blake, A. J.; Wilson, C.; McMaster, J.; Arnold, P. L. Titanium(IV) Alkoxy-N-heterocyclic Carbenes: Structural Preferences of Alkoxide and Bromide Adducts. *Organometallics* **2006**, *25* (8), 1861−1867.
(67) Srivastava, R.; Moneuse, R.; Petit, J.; Pavard, P.-A.; Dardun, V.; Rivat, M.; Schiltz, P.; Solari, M.; Jeanneau, E.; Veyre, L.; Thieuleux, C.; Quadrelli, E. A.; Camp, C. Early/Late Heterobimetallic Tantalum/Rhodium Species Assembled Through a Novel Bifunctional NHC-OH Ligand. *Chem. - Eur. J.* **2018**, *24* (17), 4361−4370.
(68) Srivastava, R.; Quadrelli, E. A.; Camp, C. Lability of Ta-NHC adducts as a synthetic route towards heterobimetallic Ta/Rh complexes. *Dalton Trans.* **2020**, *49* (10), 3120−3128.
(69) Aihara, H.; Matsuo, T.; Kawaguchi, H. Titanium N-heterocyclic carbene complexes incorporating an imidazolium-linked bis(phenol). *Chem. Commun.* **2003**, *17*, 2204−2205.
(70) Zhang, D.; Aihara, H.; Watanabe, T.; Matsuo, T.; Kawaguchi, H. Zirconium complexes of the tridentate bis(aryloxide)-N-heterocyclic-carbene ligand: Chloride and alkyl functionalized derivatives. *J. Organomet. Chem.* **2007**, *692* (1−3), 234−242.
(71) Zhang, D.; Kawaguchi, H. Deprotonation Attempts on Imidazolium Salt Tethered by Substituted Phenol and Construction of Its Magnesium Complex by Transmetalation. *Organometallics* **2006**, *25* (22), 5506−5509.
(72) Kerr, R. W. F.; Ewing, P. M. D. A.; Raman, S. K.; Smith, A. D.; Williams, C. K.; Arnold, P. L. Ultrarapid Cerium(III)−NHC Catalysts for High Molar Mass Cyclic Polylactide. *ACS Catal.* **2021**, *11* (3), 1563−1569.
(73) Casely, I. J.; Liddle, S. T.; Blake, A. J.; Wilson, C.; Arnold, P. L. Tetravalent cerium carbene complexes. *Chem. Commun.* **2007**, *47*, 5037−5039.
(74) Arnold, P. L.; Liddle, S. T.; McMaster, J.; Jones, C.; Mills, D. P. A lanthanide-gallium complex stabilized by the N-heterocyclic carbene group. *J. Am. Chem. Soc.* **2007**, *129* (17), 5360−5361.
(75) Arnold, P. L.; Casely, I. J. F-block N-heterocyclic carbene complexes. *Chem. Rev.* **2009**, *109* (8), 3599−3611.
(76) Arnold, P. L.; Cadenbach, T.; Marr, I. H.; Fyfe, A. A.; Bell, N. L.; Bellabarba, R.; Tooze, R. P.; Love, J. B. Homo- and heteroleptic alkoxycarbene f-element complexes and their reactivity towards acidic N-H and C-H bonds. *Dalton Trans.* **2014**, *43* (38), 14346−14358.
(77) Liddle, S. T.; Edworthy, I. S.; Arnold, P. L. Anionic tethered N-heterocyclic carbene chemistry. *Chem. Soc. Rev.* **2007**, *36* (11), 1732−1744.
(78) Turner, Z. R.; Bellabarba, R.; Tooze, R. P.; Arnold, P. L. Addition-elimination reactions across the M-C bond of metal N-heterocyclic carbenes. *J. Am. Chem. Soc.* **2010**, *132* (12), 4050−4051.
(79) Arnold, P. L.; Kerr, R. W. F.; Weetman, C.; Docherty, S. R.; Rieb, J.; Cruickshank, F. L.; Wang, K.; Jandl, C.; McMullon, M. W.; Pöthig, A.; Kühn, F. E.; Smith, A. D. Selective and catalytic carbon dioxide and heteroallene activation mediated by cerium N-heterocyclic carbene complexes. *Chem. Sci.* **2018**, *9* (42), 8035−8045.
(80) Gu, X.; Zhang, L.; Zhu, X.; Wang, S.; Zhou, S.; Wei, Y.; Zhang, G.; Mu, X.; Huang, Z.; Hong, D.; Zhang, F. Synthesis of Bis(NHC)-Based CNC-Pincer Rare-Earth-Metal Amido Complexes and Their Application for the Hydrophosphination of Heterocumulenes. *Organometallics* **2015**, *34* (18), 4553−4559.
(81) DeJesus, J. F.; Kerr, R. W. F.; Penchoff, D. A.; Carroll, X. B.; Peterson, C. C.; Arnold, P. L.; Jenkins, D. M. Actinide tetra-N-heterocyclic carbene 'sandwiches'. *Chem. Sci.* **2021**, *12* (22), 7882−7887.
(82) Garner, M. E.; Hohloch, S.; Maron, L.; Arnold, J. A New Supporting Ligand in Actinide Chemistry Leads to Reactive Bis(NHC)borate-Supported Thorium Complexes. *Organometallics* **2016**, *35* (17), 2915−2922.
(83) Garner, M. E.; Parker, B. F.; Hohloch, S.; Bergman, R. G.; Arnold, J. Thorium Metallacycle Facilitates Catalytic Alkyne Hydrophosphination. *J. Am. Chem. Soc.* **2017**, *139* (37), 12935−12938.
(84) Garner, M. E.; Hohloch, S.; Maron, L.; Arnold, J. Carbon-Nitrogen Bond Cleavage by a Thorium-NHC-bpy Complex. *Angew. Chem., Int. Ed.* **2016**, *55* (44), 13789−13792.
(85) Pankhurst, J. R.; Hohloch, S. N-heterocyclic and mesoionic carbene complexes of the actinides. *Comprehensive Organometallic Chemistry IV*; Elsevier: Amsterdam, 2021.
(86) Arnold, P. L.; Casely, I. J.; Turner, Z. R.; Carmichael, C. D. Functionalised saturated-backbone carbene ligands: yttrium and uranyl alkoxy-carbene complexes and bicyclic carbene-alcohol adducts. *Chem. - Eur. J.* **2008**, *14* (33), 10415−10422.

https://doi.org/10.1021/acs.inorgchem.1c02087
Inorg. Chem. 2021, 60, 15421−15434

(87) Langeslay, R. R.; Kaphan, D. M.; Marshall, C. L.; Stair, P. C.; Sattelberger, A. P.; Delferro, M. Catalytic Applications of Vanadium: A Mechanistic Perspective. *Chem. Rev.* **2019**, *119* (4), 2128−2191.
(88) Tran, B. L.; Pinter, B.; Nichols, A. J.; Konopka, F. T.; Thompson, R.; Chen, C.-H.; Krzystek, J.; Ozarowski, A.; Telser, J.; Baik, M.-H.; Meyer, K.; Mindiola, D. J. A planar three-coordinate vanadium(II) complex and the study of terminal vanadium nitrides from N2: a kinetic or thermodynamic impediment to N-N bond cleavage? *J. Am. Chem. Soc.* **2012**, *134* (31), 13035−13045.
(89) Grant, L. N.; Krzystek, J.; Pinter, B.; Telser, J.; Grützmacher, H.; Mindiola, D. J. Finding a soft spot for vanadium: a P-bound OCP ligand. *Chem. Commun.* **2019**, *55* (42), 5966−5969.
(90) Tran, B. L.; Thompson, R.; Ghosh, S.; Gao, X.; Chen, C.-H.; Baik, M.-H.; Mindiola, D. J. A four-coordinate thionitrosyl complex of vanadium. *Chem. Commun.* **2013**, *49* (27), 2768−2770.
(91) Tran, B. L.; Singhal, M.; Park, H.; Lam, O. P.; Pink, M.; Krzystek, J.; Ozarowski, A.; Telser, J.; Meyer, K.; Mindiola, D. J. Reactivity Studies of a Masked Three-Coordinate Vanadium(II) Complex. *Angew. Chem.* **2010**, *122* (51), 10067−10071.
(92) Cummins, C. C. Terminal, anionic carbide, nitride, and phosphide transition-metal complexes as synthetic entries to low-coordinate phosphorus derivatives. *Angew. Chem., Int. Ed.* **2006**, *45* (6), 862−870.
(93) Stinghen, D.; Atzori, M.; Fernandes, C. M.; Ribeiro, R. R.; de Sa, E. L.; Back, D. F.; Giese, S. O. K.; Hughes, D. L.; Nunes, G. G.; Morra, E.; Chiesa, M.; Sessoli, R.; Soares, J. F. A Rare Example of Four-Coordinate Nonoxido Vanadium(IV) Alkoxide in the Solid State: Structure, Spectroscopy, and Magnetization Dynamics. *Inorg. Chem.* **2018**, *57* (18), 11393−11403.
(94) Carroll, T. G.; Garwick, R.; Wu, G.; Ménard, G. A Mono-, Di-, and Trivanadocene Phosphorus Oxide Series: Synthesis, Magnetism, and Chemical/Electrochemical Properties. *Inorg. Chem.* **2018**, *57* (18), 11543−11551.
(95) Ferrando-Soria, J.; Vallejo, J.; Castellano, M.; Martínez-Lillo, J.; Pardo, E.; Cano, J.; Castro, I.; Lloret, F.; Ruiz-García, R.; Julve, M. Molecular magnetism, quo vadis? A historical perspective from a coordination chemist viewpoint☆. *Coord. Chem. Rev.* **2017**, *339*, 17−103.
(96) Freitag, K.; Stennett, C. R.; Mansikkamäki, A.; Fischer, R. A.; Power, P. P. Two-Coordinate, Nonlinear Vanadium(II) and Chromium(II) Complexes of the Silylamide Ligand-N(SiMePh2)2: Characterization and Confirmation of Orbitally Quenched Magnetic Moments in Complexes with Sub-d5 Electron Configurations. *Inorg. Chem.* **2021**, *60* (6), 4108−4115.
(97) Albino, A.; Benci, S.; Tesi, L.; Atzori, M.; Torre, R.; Sanvito, S.; Sessoli, R.; Lunghi, A. First-Principles Investigation of Spin-Phonon Coupling in Vanadium-Based Molecular Spin Quantum Bits. *Inorg. Chem.* **2019**, *58* (15), 10260−10268.
(98) Fataftah, M. S.; Bayliss, S. L.; Laorenza, D. W.; Wang, X.; Phelan, B. T.; Wilson, C. B.; Mintun, P. J.; Kovos, B. D.; Wasielewski, M. R.; Han, S.; Sherwin, M. S.; Awschalom, D. D.; Freedman, D. E. Trigonal Bipyramidal V3+ Complex as an Optically Addressable Molecular Qubit Candidate. *J. Am. Chem. Soc.* **2020**, *142* (48), 20400−20408.
(99) Jain, S. K.; Yu, C.-J.; Wilson, C. B.; Tabassum, T.; Freedman, D. E.; Han, S. Dynamic Nuclear Polarization with Vanadium(IV) Metal Centers. *Chem.* **2021**, *7* (2), 421−435.
(100) Zadrozny, J. M.; Niklas, J.; Poluektov, O. G.; Freedman, D. E. Multiple Quantum Coherences from Hyperfine Transitions in a Vanadium(IV) Complex. *J. Am. Chem. Soc.* **2014**, *136* (45), 15841−15844.
(101) Herrmann, W. A.; Öfele, K.; Elison, M.; Kühn, F. E.; Roesky, P. W. Nucleophilic cyclocarbenes as ligands in metal halides and metal oxides. *J. Organomet. Chem.* **1994**, *480* (1−2), c7−c9.
(102) Abernethy, C. D.; Codd, G. M.; Spicer, M. D.; Taylor, M. K. A highly stable N-heterocyclic carbene complex of trichloro-oxo-vanadium(V) displaying novel Cl-Ccarbene bonding interactions. *J. Am. Chem. Soc.* **2003**, *125* (5), 1128−1129.
(103) Zhang, W.; Nomura, K. Facile Synthesis of (Imido)vanadium-(V)−Alkyl, Alkylidene Complexes Containing an N-Heterocyclic Carbene Ligand from Their Trialkyl Analogues. *Organometallics* **2008**, *27* (24), 6400−6402.
(104) Igarashi, A.; Kolychev, E. L.; Tamm, M.; Nomura, K. Synthesis of (Imido)Vanadium(V) Dichloride Complexes Containing Anionic N-Heterocyclic Carbenes That Contain a Weakly Coordinating Borate Moiety: New MAO-Free Ethylene Polymerization Catalysts. *Organometallics* **2016**, *35* (11), 1778−1784.
(105) Nomura, K.; Nagai, G.; Izawa, I.; Mitsudome, T.; Tamm, M.; Yamazoe, S. XAS Analysis of Reactions of (Arylimido)vanadium(V) Dichloride Complexes Containing Anionic NHC That Contains a Weakly Coordinating B(C6F5)3 Moiety (WCA-NHC) or Phenoxide Ligands with Al Alkyls: A Potential Ethylene Polymerization Catalyst with WCA-NHC Ligands. *ACS omega* **2019**, *4* (20), 18833−18845.
(106) Zhang, S.; Zhang, W.-C.; Shang, D.-D.; Wu, Y.-X. Synthesis of ultra-high-molecular-weight ethylene-propylene copolymer via quasi-living copolymerization with N -heterocyclic carbene ligated vanadium complexes. *J. Polym. Sci., Part A: Polym. Chem.* **2019**, *57* (4), 553−561.
(107) Hatagami, K.; Nomura, K. Synthesis of (Adamantylmido)-vanadium(V)-Alkyl, Alkylidene Complex Trapped with PMe 3: Reactions of the Alkylidene Complexes with Phenols. *Organometallics* **2014**, *33* (22), 6585−6592.
(108) Zhang, S.; Tamm, M.; Nomura, K. 1,2-C−H Activation of Benzene Promoted by (Arylimido)vanadium(V)-Alkylidene Complexes: Isolation of the Alkylidene, Benzyne Complexes. *Organometallics* **2011**, *30* (10), 2712−2720.
(109) Johnson, C. E.; Kysor, E. A.; Findlater, M.; Jasinski, J. P.; Metell, A. S.; Queen, J. W.; Abernethy, C. D. The synthesis and characterization of IMesH(+)(eta(3)-C(5)H(5))V(N)Cl(2)(−): An anionic vanadium(v) complex with a terminal nitrido ligand. *Dalton Trans.* **2010**, *39* (14), 3482−3488.
(110) Weetman, C.; Notman, S.; Arnold, P. L. Destruction of chemical warfare agent simulants by air and moisture stable metal NHC complexes. *Dalton Trans.* **2018**, *47* (8), 2568−2574.
(111) Lorber, C.; Vendier, L. Synthesis and structure of early transition metal NHC complexes. *Dalton Trans.* **2009**, *35*, 6972−6984.
(112) Downing, S. P.; Guadaño, S. C.; Pugh, D.; Danopoulos, A. A.; Bellabarba, R. M.; Hanton, M.; Smith, D.; Tooze, R. P. Indenyl- and Fluorenyl-Functionalized N-Heterocyclic Carbene Complexes of Titanium, Zirconium, Vanadium, Chromium, and Yttrium. *Organometallics* **2007**, *26* (15), 3762−3770.
(113) Pugh, D.; Wright, J. A.; Freeman, S.; Danopoulos, A. A. 'Pincer' dicarbene complexes of some early transition metals and uranium. *Dalton Trans.* **2006**, *6*, 775−782.
(114) McGuinness, D. S.; Gibson, V. C.; Steed, J. W. Bis(carbene)-pyridine Complexes of the Early to Middle Transition Metals: Survey of Ethylene Oligomerization and Polymerization Capability. *Organometallics* **2004**, *23* (26), 6288−6292.
(115) Romain, C.; Specklin, D.; Miqueu, K.; Sotiropoulos, J.-M.; Fliedel, C.; Bellemin-Laponnaz, S.; Dagorne, S. Unusual Benzyl Migration Reactivity in NHC-Bearing Group 4 Metal Chelates: Synthesis, Characterization, and Mechanistic Investigations. *Organometallics* **2015**, *34* (20), 4854−4863.
(116) Romain, C.; Fliedel, C.; Bellemin-Laponnaz, S.; Dagorne, S. NHC Bis-Phenolate Aluminum Chelates: Synthesis, Structure, and Use in Lactide and Trimethylene Carbonate Polymerization. *Organometallics* **2014**, *33* (20), 5730−5739.
(117) Dagorne, S.; Bellemin-Laponnaz, S.; Romain, C. Neutral and Cationic N-Heterocyclic Carbene Zirconium and Hafnium Benzyl Complexes: Highly Regioselective Oligomerization of 1-Hexene with a Preference for Trimer Formation. *Organometallics* **2013**, *32* (9), 2736−2743.
(118) Suresh, L.; Finnstad, J.; Törnroos, K. W.; Le Roux, E. Bis(phenolate)-functionalized N-heterocyclic carbene complexes of oxo- and imido-vanadium(V). *Inorg. Chim. Acta* **2021**, *521*, 120301.

https://doi.org/10.1021/acs.inorgchem.1c02087
Inorg. Chem. 2021, 60, 15421−15434

(119) We would like to note that contrary to the reported procedure by LeRoux and co-workers (ref 118), in our case indiffferently from the ligand batch, solvent, and $VO(O^iPr)_3$ source used, we only obtained clean material, if a slight excess of $VO(O^iPr)_3$ (1.2 equiv) was used.
(120) LeRoux and co-workers (ref 118) reported a chemical shift of −513 ppm for this compound.
(121) Basuli, F.; Kilgore, U. J.; Hu, X.; Meyer, K.; Pink, M.; Huffman, J. C.; Mindiola, D. J. Cationic and neutral four-coordinate alkylidene complexes of vanadium(IV) containing short V═C bonds. *Angew. Chem., Int. Ed.* **2004**, *43* (24), 3156−3159.
(122) Neese, F. Software update: the ORCA program system, version 4.0. *Wiley Interdiscip. Rev.: Comput. Mol. Sci.* **2018**, *8*, 1.
(123) Neese, F. The ORCA program system. *Wiley Interdiscip. Rev.: Comput. Mol. Sci.* **2012**, *2* (1), 73−78.
(124) Grimme, S.; Ehrlich, S.; Goerigk, L. Effect of the damping function in dispersion corrected density functional theory. *J. Comput. Chem.* **2011**, *32* (7), 1456−1465.
(125) Grimme, S.; Antony, J.; Ehrlich, S.; Krieg, H. A consistent and accurate ab initio parametrization of density functional dispersion correction (DFT-D) for the 94 elements H-Pu. *J. Chem. Phys.* **2010**, *132* (15), 154104.
(126) Perdew. Density-functional approximation for the correlation energy of the inhomogeneous electron gas. *Phys. Rev. B: Condens. Matter Mater. Phys.* **1986**, *33* (12), 8822−8824.
(127) Perdew; Burke; Ernzerhof. Generalized Gradient Approximation Made Simple. *Phys. Rev. Lett.* **1996**, *77* (18), 3865−3868.
(128) Weigend, F.; Ahlrichs, R. Balanced basis sets of split valence, triple zeta valence and quadruple zeta valence quality for H to Rn: Design and assessment of accuracy. *Phys. Chem. Chem. Phys.* **2005**, *7* (18), 3297−3305.
(129) Pantazis, D. A.; Chen, X.-Y.; Landis, C. R.; Neese, F. All-Electron Scalar Relativistic Basis Sets for Third-Row Transition Metal Atoms. *J. Chem. Theory Comput.* **2008**, *4* (6), 908−919.
(130) van Lenthe, E.; Baerends, E. J.; Snijders, J. G. Relativistic regular two-component Hamiltonians. *J. Chem. Phys.* **1993**, *99* (6), 4597−4610.
(131) van Wüllen, C. Molecular density functional calculations in the regular relativistic approximation: Method, application to coinage metal diatomics, hydrides, fluorides and chlorides, and comparison with first-order relativistic calculations. *J. Chem. Phys.* **1998**, *109* (2), 392−399.
(132) Weigend, F. Accurate Coulomb-fitting basis sets for H to Rn. *Phys. Chem. Chem. Phys.* **2006**, *8* (9), 1057−1065.
(133) For a thorough investigation of related LLCTs in a bis-triazolylidene carbazolid, please see ref 29.
(134) Nomura, K.; Schrock, R. R.; Davis, W. M. Synthesis of Vanadium(III), -(IV), and -(V) Complexes That Contain the Pentafluorophenyl-Substituted Triamidoamine Ligand [(C 6 F 5 NCH 2 CH 2) 3 N] 3-. *Inorg. Chem.* **1996**, *35* (12), 3695−3701.
(135) Moriuchi, T.; Beppu, T.; Ishino, K.; Nishina, M.; Hirao, T. Structural Control of (Arylimido)vanadium(V) Compounds through π Conjugation. *Eur. J. Inorg. Chem.* **2008**, *2008* (12), 1969−1973.
(136) Wu, Y.; Wang, S.; Zhu, X.; Yang, G.; Wei, Y.; Zhang, L.; Song, H. Synthesis, characterization, and catalytic activity of rare earth metal amides supported by a diamido ligand with a CH2SiMe2 link. *Inorg. Chem.* **2008**, *47* (12), 5503−5511.
(137) Zhu, X.; Fan, J.; Wu, Y.; Wang, S.; Zhang, L.; Yang, G.; Wei, Y.; Yin, C.; Zhu, H.; Wu, S.; Zhang, H. Synthesis, Characterization, Selective Catalytic Activity, and Reactivity of Rare Earth Metal Amides with Different Metal−Nitrogen Bonds. *Organometallics* **2009**, *28* (13), 3882−3888.
(138) Liu, Q.; Guo, Z.; Han, H.; Tong, H.; Wei, X. Lithium, magnesium, zinc complexes supported by tridentate pincer type pyrrolyl ligands: Synthesis, crystal structures and catalytic activities for the cyclotrimerization of isocyanates. *Polyhedron* **2015**, *85*, 15−19.
(139) Wang, H.-M.; Li, H.-X.; Yu, X.-Y.; Ren, Z.-G.; Lang, J.-P. Cyclodimerization and cyclotrimerization of isocyanates promoted by one praseodymium benzenethiolate complex [Pr(SPh)3(THF)3]. *Tetrahedron* **2011**, *67* (8), 1530−1535.
(140) Sharpe, H. R.; Geer, A. M.; Williams, H. E. L.; Blundell, T. J.; Lewis, W.; Blake, A. J.; Kays, D. L. Cyclotrimerisation of isocyanates catalysed by low-coordinate Mn(ii) and Fe(ii) m-terphenyl complexes. *Chem. Commun.* **2017**, *53* (5), 937−940.
(141) Duong, H. A.; Cross, M. J.; Louie, J. N-heterocyclic carbenes as highly efficient catalysts for the cyclotrimerization of isocyanates. *Org. Lett.* **2004**, *6* (25), 4679−4681.
(142) Li, C.; Zhao, W.; He, J.; Zhang, Y. Highly efficient cyclotrimerization of isocyanates using N-heterocyclic olefins under bulk conditions. *Chem. Commun.* **2019**, *55* (83), 12563−12566.
(143) Liu, S.; Amaro-Estrada, J. I.; Baltrun, M.; Douair, I.; Schoch, R.; Maron, L.; Hohloch, S. Catalytic Deoxygenation of Nitroarenes Mediated by High-Valent Molybdenum(VI)−NHC Complexes. *Organometallics* **2021**, *40* (2), 107−118.
(144) Baltrun, M.; Watt, F. A.; Schoch, R.; Hohloch, S. Dioxo-, Oxo-imido-, and Bis-imido-Molybdenum(VI) Complexes with a Bis-phenolate-NHC Ligand. *Organometallics* **2019**, *38* (19), 3719−3729.
(145) Telser, J.; Wu, C.-C.; Chen, K.-Y.; Hsu, H.-F.; Smirnov, D.; Ozarowski, A.; Krzystek, J. Aminocarboxylate complexes of vanadium-(III): Electronic structure investigation by high-frequency and -field electron paramagnetic resonance spectroscopy. *J. Inorg. Biochem.* **2009**, *103* (4), 487−495.
(146) Kurogi, T.; Manor, B. C.; Carroll, P. J.; Mindiola, D. J. Trimethylsilyl imide complexes of tantalum: Can the silyl group be eliminated? *Polyhedron* **2017**, *125*, 80−85.
(147) Hohloch, S.; Kriegel, B. M.; Bergman, R. G.; Arnold, J. Group 5 chemistry supported by β-diketiminate ligands. *Dalton Trans.* **2016**, *45* (40), 15725−15745.
(148) Downing, S. P.; Danopoulos, A. A. Indenyl- and Fluorenyl-Functionalized N -Heterocyclic Carbene Complexes of Titanium and Vanadium. *Organometallics* **2006**, *25* (6), 1337−1340.
(149) Kawakita, K.; Beaumier, E. P.; Kakiuchi, Y.; Tsurugi, H.; Tonks, I. A.; Mashima, K. Bis(imido)vanadium(V)-Catalyzed 2 + 2+1 Coupling of Alkynes and Azobenzenes Giving Multisubstituted Pyrroles. *J. Am. Chem. Soc.* **2019**, *141* (10), 4194−4198.
(150) Helgert, T. R.; Zhang, X.; Box, H. K.; Denny, J. A.; Valle, H. U.; Oliver, A. G.; Akurathi, G.; Webster, C. E.; Hollis, T. K. Extreme π-Loading as a Design Element for Accessing Imido Ligand Reactivity. A CCC-NHC Pincer Tantalum Bis(imido) Complex: Synthesis, Characterization, and Catalytic Oxidative Amination of Alkenes. *Organometallics* **2016**, *35* (20), 3452−3460.
(151) Hohloch, S.; Sarkar, B.; Nauton, L.; Cisnetti, F.; Gautier, A. Are Cu(I)-mesoionic NHC carbenes associated with nitrogen additives the best Cu-carbene catalysts for the azide−alkyne click reaction in solution? A case study. *Tetrahedron Lett.* **2013**, *54* (14), 1808−1812.
(152) Watt, F. A.; Krishna, A.; Golovanov, G.; Ott, H.; Schoch, R.; Wölper, C.; Neuba, A. G.; Hohloch, S. Monoanionic Anilidophosphine Ligand in Lanthanide Chemistry: Scope, Reactivity, and Electrochemistry. *Inorg. Chem.* **2020**, *59* (5), 2719−2732.
(153) Liao, Y.; Lu, Q.; Chen, G.; Yu, Y.; Li, C.; Huang, X. Rhodium-Catalyzed Azide−Alkyne Cycloaddition of Internal Ynamides: Regioselective Assembly of 5-Amino-Triazoles under Mild Conditions. *ACS Catal.* **2017**, *7* (11), 7529−7534.
(154) Mamidyala, S. K.; Cooper, M. A. Probing the reactivity of o-phthalaldehydic acid/methyl ester: synthesis of N-isoindolinones and 3-arylaminophthalides. *Chem. Commun.* **2013**, *49* (75), 8407−8409.
(155) Stoll, S.; Schweiger, A. EasySpin, a comprehensive software package for spectral simulation and analysis in EPR. *J. Magn. Reson.* **2006**, *178* (1), 42−55.
(156) Sheldrick, G. M. SHELXT - integrated space-group and crystal-structure determination. *Acta Crystallogr., Sect. A: Found. Adv.* **2015**, *71* (1), 3−8.
(157) Dolomanov, O. V.; Bourhis, L. J.; Gildea, R. J.; Howard, J.; Puschmann, H. OLEX2: a complete structure solution, refinement and analysis program. *J. Appl. Crystallogr.* **2009**, *42* (2), 339−341.

https://doi.org/10.1021/acs.inorgchem.1c02087
Inorg. Chem. 2021, 60, 15421−15434

(158) van der Sluis, P.; Spek, A. L. BYPASS: an effective method for the refinement of crystal structures containing disordered solvent regions. *Acta Crystallogr., Sect. A: Found. Crystallogr.* **1990**, *46* (3), 194−201.

https://doi.org/10.1021/acs.inorgchem.1c02087
Inorg. Chem. 2021, 60, 15421−15434